

Universality of modulation length (and time) exponents

Saurish Chakrabarty,¹ Vladimir Dobrosavljević,² Alexander Seidel,¹ and Zohar Nussinov^{1,3,*}

¹*Department of Physics and Center for Materials Innovation,
Washington University in St Louis, MO 63130, USA.*

²*Department of Physics and National High Magnetic Field Laboratory,
Florida State University, Tallahassee, Florida 32306, USA.*

³*Kavli Institute for Theoretical Physics, Santa Barbara, CA 93106.*

(Dated: December 25, 2018)

We study systems with a crossover parameter λ , such as the temperature T , which has a threshold value λ_* across which the correlation function changes from exhibiting fixed wavelength (or time period) modulations to continuously varying modulation lengths (or times). We report on a *new exponent*, ν_L , characterizing the universal nature of this crossover. These exponents, similar to standard correlation length exponents, are obtained from motion of the poles of the momentum (or frequency) space correlation functions in the complex k -plane (or ω -plane) as the parameter λ is varied. Near the crossover (i.e., for $\lambda \rightarrow \lambda_*$), the characteristic modulation wave-vector K_R on the variable modulation length “phase” is related to that on the fixed modulation length side, q via $|K_R - q| \propto |T - T_*|^{\nu_L}$. We find, in general, that $\nu_L = 1/2$. In some special instances, ν_L may attain other rational values. We extend this result to general problems in which the eigenvalue of an operator or a pole characterizing general response functions may attain a constant real (or imaginary) part beyond a particular threshold value, λ_* . We discuss extensions of this result to multiple other arenas. These include the axial next nearest neighbor Ising (ANNNI) model. By extending our considerations, we comment on relations pertaining not only to the modulation lengths (or times) but also to the standard correlation lengths (or times). We introduce the notion of a Josephson timescale. We comment on the presence of aperiodic “chaotic” modulations in “soft-spin” and other systems. These relate to glass type features. We discuss applications to Fermi systems – with particular application to metal to band insulator transitions, change of Fermi surface topology, divergent effective masses, Dirac systems, and topological insulators. Both regular periodic and glassy (and spatially chaotic behavior) may be found in strongly correlated electronic systems.

PACS numbers: 05.50.+q, 75.10.-b, 75.10.Hk, 75.60.Ch

I. INTRODUCTION

In complex systems, there are, in general, possibly many important length and time scales that characterize correlations. Aside from correlation lengths describing the exponential decay of correlations, in some materials there are length scales that characterize periodic spatial modulations or other properties of spatially non-uniform systems as in Fig. 1. We investigate the evolution of these length scales as a function of some parameter λ . This parameter may be the temperature, the chemical potential, or some other physical quantity relevant for description of the system being studied. To illustrate our basic premise, we will largely focus on temperature dependences of the correlation function in this work. However, with change of variables, our results are valid for any parameter that, when tuned, can take us from a phase with continuously varying modulation lengths (or times) to one in which the modulation length (or time) is pinned. The crossovers we consider are not symmetry breaking transitions. Consequences of our considerations also relate to correlation lengths as we will comment on later.

Many systems exhibit subtle changes in their correlation functions at certain special temperatures. Across a certain crossover temperature T_* , an unmodulated phase of a system may start exhibiting modulations, without the system going through a phase transition. A generalization of this occurs when modulations in a system are characterized by a fixed wavelength on one side of a crossover temperature and by continuously varying wavelengths on the other side. These are generally present whenever a system has competing interactions in which different components of the interaction kernel compete to find some optimum characteristic length scales for the system, thus forming a wealth of interesting patterns. Such patterns are present in manganites [2], pnictide [3, 4] and cuprate [5–10] superconductors, quantum Hall systems [11–13], dense nuclear matter [14, 15], magnetic systems [16–21], heavy fermion compounds [22, 23], membranes [24], cholesterols [25], magnetic garnets [26], dipolar systems [27, 28], systems with nematic phases [29], and countless other systems [30–34].

II. OUR MAIN RESULTS AND THEIR IMPLICATIONS

In this work, we report on the temperature (or other parameter) dependence of emergent modulation lengths

*Electronic address: zohar@wuphys.wustl.edu

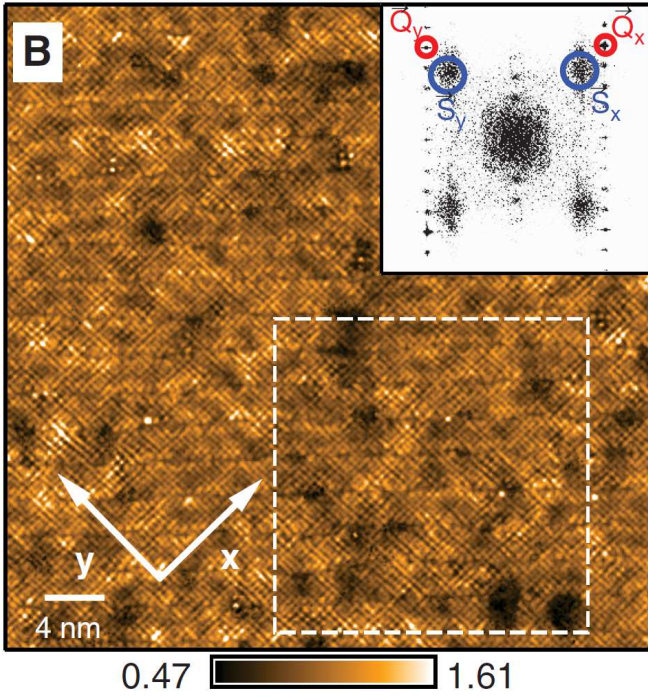


FIG. 1: Sub-unit-cell resolution image of the electronic structure of a cuprate superconductor at the pseudo-gap energy. Inset shows Fourier space image of the same figure. Nematic and smectic phases are highlighted using the red and blue circles respectively. The nematic phase is characterized by commensurate wave-vectors \vec{Q} . The smectic wave-vector, on the other hand takes incommensurate values, \vec{S} which is dependent on the amount of doping, albeit weakly. (From Ref. [1]. Reprinted with permission from AAAS.)

that govern the size of various domains present in some systems. In its simplest incarnation, our central result is that if fixed wavelength modulations characterized by a particular *finite* length-scale, L_* , appear beyond some temperature T_* then, the modulation length, L_D on the other side of the crossover differs from L_* as

$$|L_D - L_*| \propto |T - T_*|^{\nu_L}. \quad (1)$$

When there are *no modulations* on one side of T_* , i.e., $L_* \rightarrow \infty$, we have near the crossover,

$$L_D \propto |T - T_*|^{-\nu_L}. \quad (2)$$

Additionally, apart from some special situations, we find that irrespective of the interaction, $\nu_L = 1/2$. We arrive at this rather universal result assuming that there is no phase transition at the crossover temperature T_* . Our result holds everywhere inside a given thermodynamic phase of a system.

Our considerations are not limited to continuous crossovers. We discuss a corollary of our analysis to systems with discontinuous (*first order*) jumps in the correlation or modulation lengths.

We discuss the situation in which we might have a branch point at the crossover point. We present examples where we obtain rational and irrational exponents and also the anomalous critical exponent η . We discuss connections to critical scaling of correlation lengths.

Our results for length scales can be extended to timescales. We introduce the notion of a Josephson timescale.

Lastly, for completeness, we comment on the presence of phases with aperiodic “chaotic” modulations (characteristic of amorphous configurations) in systems governed by non-linear Euler-Lagrange equations. Aperiodic “chaotic” modulations may appear in strongly correlated electronic systems.

In the appendix, we present applications to Fermi systems pertaining to metal–band insulator transition, change of Fermi surface topology, divergence of effective masses, Dirac systems and topological insulators.

III. THE SYSTEMS OF STUDY

In this section, we introduce a simple form of the system we study which involves classical scalar spins/fields. We consider a translationally invariant system on a lattice whose Hamiltonian is given by

$$H = \frac{1}{2} \sum_{\vec{x} \neq \vec{y}} V(|\vec{x} - \vec{y}|) S(\vec{x}) S(\vec{y}). \quad (3)$$

The quantities $\{S(\vec{x})\}$ portray classical scalar spins or fields. The sites \vec{x} and \vec{y} lie on a hyper-cubic (or some other) lattice with N sites having unit lattice constant (In the quantum arena, we replace the spins $\vec{S}(\vec{x})$ in Eq. (3) by Fermi or Bose or quantum spin operators).

The results that will be derived in this work apply to a variety of systems. These include systems with n -component spins or fields, both classical and quantum. In the bulk of this work, the Hamiltonian has a bilinear form in the spins. However, later on we comment on implications to “soft” spins, wherein the “softness” is incorporated by a local quartic term in the Hamiltonian. For example, the n -component spin system whose Hamiltonian is given by

$$H = \frac{1}{2} \sum_{\vec{x} \neq \vec{y}} V(|\vec{x} - \vec{y}|) \vec{S}(\vec{x}) \cdot \vec{S}(\vec{y}) + \frac{u}{4} \sum_{\vec{x}} \left(\vec{S}(\vec{x}) \cdot \vec{S}(\vec{x}) - n \right)^2, \quad (4)$$

represents “hard” spin or $O(n)$ systems if $u \gg 1$ as this enforces the “hard” normalization constraint, $\vec{S}(\vec{x}) \cdot \vec{S}(\vec{x}) = n$. It represents “soft”-spin systems for finite (or small) u . Effects of such higher order terms will be discussed later.

We will also discuss the evolution of general correlation functions in systems in which the exact form of the Hamiltonian might not be known.

In what follows, $v(k)$ and $s(\vec{k})$ will denote the Fourier transforms of $V(|\vec{x}-\vec{y}|)$ and $S(\vec{x})$. The Fourier transform convention used here is that

$$a(\vec{k}) = \sum_{\vec{x}} A(\vec{x}) e^{i\vec{k}\cdot\vec{x}}, \text{ and,} \\ A(\vec{x}) = \frac{1}{N} \sum_{\vec{k}} a(\vec{k}) e^{-i\vec{k}\cdot\vec{x}}. \quad (5)$$

We have,

$$H = \frac{1}{2N} \sum_{\vec{k}} v(k) |s(\vec{k})|^2. \quad (6)$$

For analytic interactions, $v(k)$ is a function of k^2 (to avoid branch cuts). The two point correlation function for the system in Eq. (3) is, $G(\vec{x}) = \langle S(0)S(\vec{x}) \rangle$. For large distances, the correlation function typically behaves as

$$G(x) \approx \sum_i f_i(x) \cos\left(\frac{2\pi x}{L_D^{(i)}}\right) e^{-x/\xi_i}, \quad (7)$$

where for the i -th term, $f_i(x)$ is an algebraic prefactor, $L_D^{(i)}$ is the modulation length and ξ_i is the corresponding correlation length. In general, the function $f_i(x)$ may contain a factor with an anomalous exponent η (usually not an integer), such as, $f_i(x) \propto 1/x^{d-2+\eta}$. Most of our results are derived assuming the absence of such behavior, i.e., $\eta = 0$. However, we will comment later about situations with non-zero η . Generally there can be multiple correlation and modulation lengths. In the Fourier space, $G(\vec{k}) = \frac{1}{N} \langle |s(\vec{k})|^2 \rangle$. The modulation and correlation lengths can be obtained respectively from the real and imaginary parts of the poles of $G(\vec{k})$ in the complex k -plane.

General considerations: Correlation and modulation lengths from momentum space correlation function

The correlation function $G(\vec{x})$ in (d -dimensional) real space is related to the momentum space correlation function $G(\vec{k})$ by

$$G(\vec{x}) = \int \frac{d^d k}{(2\pi)^d} G(\vec{k}) e^{-i\vec{k}\cdot\vec{x}}. \quad (8)$$

On the lattice, the integral above must be replaced by summation over \vec{k} -values belonging to the first Brillouin zone. In the continuum, which we discuss here, the integral range is unbounded. Even in lattice systems, doing an unbounded summation over \vec{k} -values provides a good approximation for the correlation function in real space in many scenarios.

For spherically symmetric problems, i.e., when $G(\vec{k}) = G(k)$,

$$G(x) = \int_0^\infty \frac{k^{d-1} dk}{(2\pi)^{d/2}} \frac{J_{d/2-1}(kx)}{(kx)^{d/2-1}} G(k), \quad (9)$$

where $J_\nu(x)$ is a Bessel function of order ν . The above integral can be evaluated by choosing an appropriate contour in the complex k -plane. The contour can be closed along a circular arc of radius $R \rightarrow \infty$ provided

$$|G(k)| \lesssim k^{-\frac{d+1}{2}}, \text{ as } k \rightarrow \infty. \quad (10)$$

In evaluating the integral in Eq. (9) we obtain contributions from residues associated with the poles of the integrand as well as contributions from its branch points. We use $K = K_R + iK_I$ to represent the poles and branch points of the integrand in the complex plane. The correlation and modulation lengths in the system are determined respectively by the imaginary (K_I) and real parts (K_R) of these poles and branch points. Together, all these singularities could be summarized using,

$$\boxed{\frac{1}{G^{(m)}(K)} = 0}, \quad (11)$$

where $0 \leq m < \infty$ is the order of the smallest order derivative of $G(k)$ which diverges at $k = K$. [Note: $m = 0$ if $G(k)$ has a pole of finite order at $k = K$, and $m \geq 0$ for the branch points.]

For a comment on the situation in which the function $G(T, k)$ is an entire function of k (analytic everywhere) see footnote [35].

IV. A UNIVERSAL DOMAIN LENGTH EXPONENT – DETAILS OF ANALYSIS

Here, we derive (via various inter-related approaches), our main finding of a new exponent for the domain length in rather general systems. Our result below applies to *general fields* [real or complex scalar fields, vectorial (or tensorial) fields of both the discrete (e.g., Potts like) and continuous variants]. The characteristic length scales of the system governed by the poles of the correlation function wherein $G^{-1}(T, k) = 0$, where $G^{-1}(T, k)$ denotes the reciprocal of the Fourier transformed pair correlator calculated for a complex wave-vector k at a temperature T . We will now consider the situation in which the system exhibits modulations at a fixed wave-vector q for a finite range of temperatures on one side of T_* , [viz., (i) $T > T_*$, or, (ii) $T < T_*$] and starts to exhibit variable wavelength modulations on the other side [(iii) $T < T_*$ for (i) and $T > T_*$ for (ii)]. A schematic illustrating this is shown in Fig. 2. In sub-section IV A, we assume that the pair correlation function is meromorphic (realized physically by *absence of phase transitions*) at the crossover point and illustrate how modulation length exponents may appear. In sub-section IV B, we will comment on the situation where the crossover point may be a branch point of the correlation function.

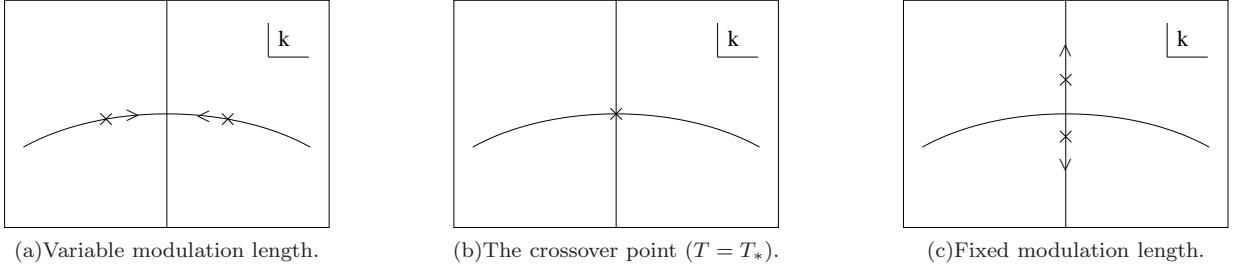


FIG. 2: Schematic showing the trajectories of the singularities of the correlation function near a fixed – variable modulation length crossover. Two poles of the correlation function merge at $k = k_*$ at $T = T_*$. On the fixed modulation length side of the crossover point, $\text{Re } k = q$.

A. Crossovers at general points in the complex k -plane

We will assume that the pair correlator, $G(T, k)$ is a meromorphic function of k and T near a crossover point. Our analysis below is exact as long as we do not cross any phase boundaries. Such a case is indeed materialized in the incommensurate-commensurate crossovers in the three-dimensional axial next-nearest-neighbor Ising (ANNNI) model [36, 37] (which is of type (ii) in the classification above). This phenomenon is also seen in the ground state phase diagram of Frenkel-Kontorova models [38] in which one of the coupling constants is tuned instead of temperature.

In the following two sections, we present two alternative approaches to derive a universal exponent characterizing this crossover.

1. First approach

In general, if the pair correlation function $G(T, k)$ is a meromorphic function of the temperature T and the wave-vector k near a crossover point (T_*, k_*) , then $G^{-1}(T, k)$ must have a Taylor series expansion about that point. We have,

$$G^{-1}(T, k) = \sum_{m_1, m_2=0}^{\infty} A_{m_1 m_2} (T - T_*)^{m_1} (k - k_*)^{m_2}. \quad (12)$$

Since $G^{-1}(T_*, k_*) = 0$, we have, $A_{00} = 0$. Let us try to find the trajectory of the pole $K(T)$ (with $K(T_*) = k_*$) of $G(T, k)$ in the complex k -plane as the temperature is varied around T_* . Writing down the leading terms of $G^{-1}(T, k)$, we have, in general,

$$G^{-1}(T, k) \sim \sum_{p=0}^{\lfloor m/a \rfloor} (T - T_*)^{m-ap} (k - k_*)^{n+bp} + o((T - T_*)^m (k - k_*)^n), \quad (13)$$

as $(T, k) \rightarrow (T_*, k_*)$ with m, n, a, b integers, $m, n \geq 0$ and $a, b \geq 1$, $\lfloor x \rfloor$ represents the greatest integer less than or

equal to x and $o(x)$ represents terms negligible compared to x . We have,

$$K(T) \sim k_* + C(T - T_*)^{a/b}, \quad (14)$$

where C is some constant, yielding $\nu_L = a/b$. By the very definition of T_* , on one side of T_* [(i) or (ii) above], there exists at least one root [say, $K(T)$] of G^{-1} satisfying $K_R(T) = q$, where q is a constant. On the other side [(iii) above], $K_R(T) \neq q$. As such, the function $K(T)$ is non-analytic at T_* . The left hand side of Eq. (14) is therefore not analytic at $T = T_*$, implying that the right hand side cannot be analytic. This means that (a/b) cannot be an integer, which in turn implies that $b \geq 2$. Therefore, in the most common situations we might encounter,

$$\begin{aligned} G^{-1}(T, k) &\sim A(T - T_*) + B(k - k_*)^2 \\ \Rightarrow a &= 1 \text{ and } b = 2. \end{aligned} \quad (15)$$

When Fourier transforming $G(\vec{k})$ by evaluating the integral in Eqs. (8, 9) using the technique of residues, the real part of the poles (i.e., K_R) gives rise to oscillatory modulations of length $L_D = 2\pi/K_R$. If the modulation length locks its value to $2\pi/q$ on one side of the crossover point, then, on the other side, near T_* , it must behave as

$$\begin{aligned} |2\pi/L_D - q| &\propto |T - T_*|^{1/2} \\ \Rightarrow \nu_L &= 1/2. \end{aligned} \quad (16)$$

2. Second approach

In this section, we present an alternative approach to derive the universal modulation length exponent across an analytic crossover from a “phase” with fixed modulation length to one in which the modulation length is continuously varying. If the correlation function G is a meromorphic function of k , then, expanding about a zero $k_1(T)$ of G^{-1} , we have,

$$G^{-1}(T, k) = A(T) (k - k_1(T))^{m_1} G_1^{-1}(T, k), \quad (17)$$

where $G_1^{-1}(T, k)$ is an analytic function of k and $G_1^{-1}(T, k_1(T)) \neq 0$. We can do this again for the function

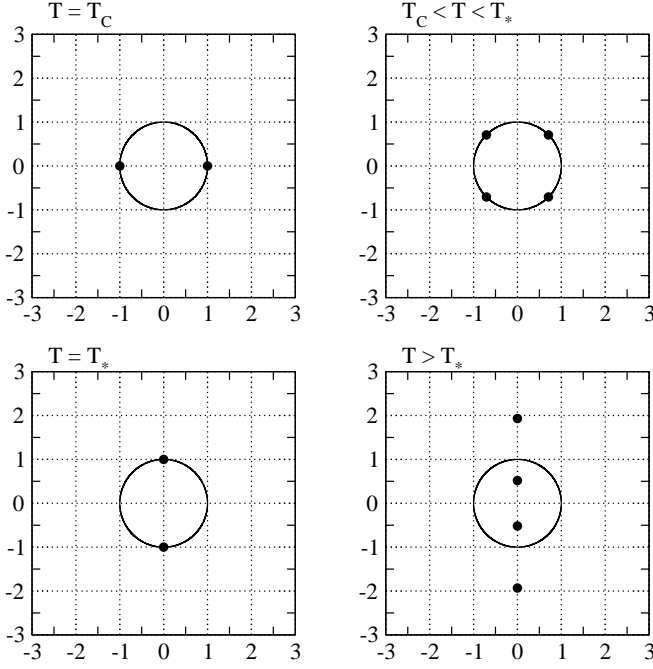


FIG. 3: Location of the poles of the correlation function of the large n Coulomb frustrated ferromagnet for $J = Q = 1$ in the complex k -plane. The circle and the Y -axis show the trajectory $K(T)$ of the poles as the temperature T is varied.

$G_1^{-1}(T, k)$ choosing one of its zeros $k_2(T)$ and continue the process until the function left over does not have any more zeros. We have,

$$G^{-1}(T, k) = A(T) \prod_{a=1}^p (k - k_a(T))^{m_a} G_p^{-1}(T, k), \quad (18)$$

where the function $G_p^{-1}(T, k)$ is an analytic function with no zeros, m_a s are integers and, in principle, p may be arbitrarily high. This factorization can be done in each phase where G is meromorphic. Let $k_1(T)$ be a non-analytic zero of G^{-1} , i.e., one for which $\text{Re } k_1(T) = q$ on one side of $T = T_*$. To ensure analyticity of G^{-1} in T in the vicinity of $T = T_*$, there must be at least one other root $k_2(T)$, such that as $T \rightarrow T_*$, both $k_1(T)$ and $k_2(T)$ veer towards k_* , where $\text{Re } k_* = q$ [e.g., see Fig. 3 which is of type (i) above, $k_* = \pm i$]. In other words, p in Eq. (18) cannot be smaller than two. The proof of this assertion is simple. If $p = 1$, then, according to Eq. (18), $G^{-1}(T, k) = A(k - k_1(T))G_1^{-1}(T, k)$. However, at $T = T_*$, $k_1(T)$ is not analytic, implying that $G^{-1}(T, k)$ can be analytic only if $p \geq 2$. For $p \geq 2$, at T_* , G^{-1} will, to leading order, vary quadratically in $(k - k_*)$ in the complex k plane near k_* . Thus,

$$\left. \frac{\partial G^{-1}}{\partial k} \right|_{(T_*, k_*)} = 0. \quad (19)$$

Now, if G^{-1} has a finite first partial derivative relative to the temperature T then, to leading order,

$$G^{-1}(T_*, k_*) + (T - T_*) \left. \frac{\partial G^{-1}}{\partial T} \right|_{(T_*, k_*)} + \frac{(k - k_*)^2}{2!} \left. \frac{\partial^2 G^{-1}}{\partial k^2} \right|_{(T_*, k_*)} = 0. \quad (20)$$

By its definition, k_* satisfies the equality $G^{-1}(T_*, k_*) = 0$. Therefore,

$$|k - k_*| = \sqrt{\frac{2(T_* - T) \left. \frac{\partial G^{-1}}{\partial T} \right|_{(T_*, k_*)}}{\left. \frac{\partial^2 G^{-1}}{\partial k^2} \right|_{(T_*, k_*)}}}. \quad (21)$$

Equation (16) is an exact equality. It shows that $\nu_L = 1/2$ *universally* unless one of $\left. \frac{\partial^2 G^{-1}}{\partial k^2} \right|_{(T_*, k_*)}$ and $\left. \frac{\partial G^{-1}}{\partial T} \right|_{(T_*, k_*)}$ vanishes at (T_*, k_*) . [39] Often, $G^{-1}(T, k)$ is a rational function of k , i.e.,

$$G^{-1}(T, k) = \frac{G_n^{-1}(T, k)}{G_d^{-1}(T, k)}, \quad (22)$$

where $G_n^{-1}(T, k)$ and $G_d^{-1}(T, k)$ are polynomial functions of k . In those instances, we get the same result as above by using $G_n^{-1}(T, k)$ in the above arguments. The value of the critical exponent is similar to that appearing for the correlation length exponent for mean-field or large n theories. It should be stressed that our result of Eq. (16) is far more general.

Lock-in of the correlation length. Apart from the crossovers across which the modulation length locks in to a fixed value, we can also have situations where the correlation length becomes constant as a crossover temperature T_{**} is crossed. If this happens, we must have the same result as before. Therefore, if the correlation length has a fixed value ξ_0 on one side ($T < T_{**}$ or $T > T_{**}$) of the crossover point, then, on the other side ($T > T_{**}$ or $T < T_{**}$, respectively), near T_{**} , it must behave as,

$$|1/\xi - 1/\xi_0| \propto |T - T_{**}|^{\nu_c}, \quad (23)$$

where, like ν_L , $\nu_c = 1/2$ apart from special situations where it may take some other rational values. Here and throughout, we use ν_c to represent the usual correlation length exponent, ν to distinguish it from the modulation length exponent ν_L .

B. Branch points

A general treatment of a situation in which the crossover point is a branch point of the inverse correlation function in the complex k -plane is beyond the scope of this work. Branch points are ubiquitous in correlation functions in both classical as well as quantum systems.

For example, in the large n rendition of a bosonic system (with a Hamiltonian of Eq. (3) and $S(x)$ representing bosonic fields), the momentum space correlation function at temperature T is given by [40, 41]

$$G(\vec{k}) = \sqrt{\frac{\mu_1}{v(\vec{k}) + \mu}} \left[n_B \left(\frac{\sqrt{\mu_1(v(\vec{k}) + \mu)}}{k_B T} \right) + \frac{1}{2} \right], \quad (24)$$

where μ_1 is a constant having dimensions of energy, μ is the chemical potential, $n_B(x) = 1/(e^x - 1)$ is the Bose distribution function and k_B is the Boltzmann's constant.

Similar forms, also including spatial modulations in $G(r)$, may also appear. We briefly discuss examples where we have a branch cut in the complex k -plane.

The one-dimensional momentum space correlation function,

$$G(k) = \frac{1}{\sqrt{(k-q)^2 + r}} + \frac{1}{\sqrt{(k+q)^2 + r}}, \quad (25)$$

reflects a position space correlation function given by

$$G(x) = \frac{2 \cos(qx) K_0(x\sqrt{r})}{\pi}, \quad (26)$$

where $K_0(\cdot)$ is a modified Bessel function. We thus get length scales corresponding to the branch points $K = \pm q \pm i\sqrt{r}$ as expected.

Similarly, the three-dimensional position space correlation function corresponding to

$$G(k) = \frac{1}{\sqrt{(k-q)^2 + r}}, \quad (27)$$

exhibits the same correlation and modulation lengths along with an algebraically decaying term for large separations. Another related $G^{-1}(k)$ involving a function of $|\vec{k}|$ (i.e., not an analytic function of k^2) was investigated earlier [42].

In general, at a critical point, the correlation function for large r in d dimensions, behaves as,

$$G(r) \propto \frac{1}{r^{d-2+\eta}}, \quad (28)$$

with η the “anomalous” exponent.

If the leading order behavior of $1/G^{(m)}(T, k)$ is algebraic near a branch point (T_*, k_*) , then we get an algebraic exponent characterizing a crossover at this point [m being the lowest order derivative of $G(k)$ which diverges at $k = k_*$ as in Eq. (11)]. That is, we have,

$$\frac{1}{G^{(m)}(T, k)} \sim A(T - T_*)^{z_1} - B(k - k_*)^{z_2} \quad \text{as } (T, k) \rightarrow (T_*, k_*). \quad (29)$$

This implies,

$$(k - k_*) \sim \left(\frac{A}{B} \right)^{1/z_2} (T - T_*)^{z_1/z_2}. \quad (30)$$

We therefore observe a length-scale exponent $\nu = z_1/z_2$ at this crossover. This could characterize a correlation length, a modulation length or both. The exponent z_1/z_2 may take *irrational* values in many situations in which the function $G^{-1}(T, k)$ is not analytic near the crossover point. Such a situation could give rise to phenomena exhibiting anomalous exponents η . For example, if we have a diverging correlation length at a critical temperature T_c , for a system with a correlation function which behaves as in Eq. (28), then, we have in Eq. (29), $z_2 = 2 - \eta$. Thus, we have,

$$\begin{aligned} |L_D - L_{Dc}| &\propto |T - T_c|^{\frac{z_1}{2-\eta}}, \\ \Rightarrow \nu_L &= \frac{z_1}{2-\eta}, \end{aligned} \quad (31)$$

where $L_{Dc} = 2\pi/|\text{Re } k_*|$, and more importantly,

$$\begin{aligned} \xi &\propto |T - T_c|^{-\frac{z_1}{2-\eta}}, \\ \Rightarrow \nu_c &= \frac{z_1}{2-\eta}. \end{aligned} \quad (32)$$

Other critical exponents could also, in principle, be calculated using hyper-scaling relations.

If $G^{-1}(T, k)$ in Eq. (11) has a Puiseux representation about the crossover point, i.e.,

$$G^{-1}(T, k) = \sum_{m=m_0}^{\infty} \sum_{p=p_0}^{\infty} a_{mp} (k - k_*)^{m/a} (T - T_*)^{p/b}, \quad (33)$$

with $a_{m_0 p_0} = 0$, where m_0 , p_0 , a and b are integers, then, the result we derived above applies to the relevant length-scale and the crossover exponent $\nu = a/b$, is again a *rational number*.

Generalizing, if $G^{-1}(T, k)$ is the ratio of two Puiseux series, we use the numerator to obtain the leading order asymptotic behavior and hence obtain a rational exponent.

C. A corollary: Discontinuity in modulation lengths implies a thermodynamic phase transition

As the wave-vectors characterizing a system are continuous at crossover points near which the inverse correlation function in Fourier space is analytic in T and k , situations where there are discontinuous (*first order*) jumps in the correlation or modulation lengths must correspond to non-analyticities in the inverse correlation function suggesting the presence of a phase transition. Thus, all commensurate-commensurate crossovers must correspond to phase transitions. For example, see the ANNNI model [43].

D. Diverging correlation length at a spinodal transition

Our \vec{k} -space analysis is valid for both annealed and quenched systems so long as translational symmetry is maintained. In particular, whenever phase transitions are “avoided” the rational exponents of Eq. (14) will appear. [40, 44, 45]

In various scenarios, we may come across situations in which there are no diverging correlation lengths even when the inverse correlation function has zeros corresponding to real values of the wave-vector. These are signatures of a first order phase transition, e.g., transition from a liquid to a crystal. If the first order phase transition is somehow avoided, then the system may enter a metastable phase and may further reach a point where the correlation length diverges. Such a point in the phase diagram is referred to as the spinodal point. If it is possible to reach this point and if the inverse correlation function is analytic there, then our analysis will be valid, thereby leading to rational exponents characterizing the divergence of the correlation length. However, there are existing works in the literature which seem to suggest that such a point may not be reachable. For example, in mode coupling theories of the glass transition, the system reaches the mode coupling transition temperature T_{MCT} at which the viscosity and relaxation times diverge and hence does not reach the point where the correlation length blows up.[46]

V. $O(n)$ SYSTEMS

The correlation function for $O(n)$ systems can be calculated exactly in both low and high temperature limits. At intermediate temperatures various crossovers and phase transitions may occur where the correlation and modulation lengths might show various interesting behavior. In this section, we discuss the low and high temperature behavior length scales characterizing $O(n)$ systems.

A. Low temperature configurations

It has been shown earlier [47] that for $O(n \geq 2)$, all ground states of a system have to be spirals (or polyspirals) of characteristic wave-vectors \vec{q}_α , given by

$$v(\vec{q}_\alpha) = -\min_{\vec{k} \in \mathbb{R}^d} v(\vec{k}), \quad (34)$$

where \mathbb{R}^d represents the set of all d -dimensional real vectors. At $T = 0$, the modulation lengths in the system are given by

$$L_D^{i,\alpha}(T=0) = 2\pi/q_{i,\alpha}, \quad (35)$$

where $i(1 \leq i \leq d)$ labels the Cartesian directions in d dimensions. This, together with Eq. (36) gives us

the high and low temperature forms of the correlation function and its associated length scales.

B. High temperatures

It is known that all systems with pair-wise interactions behave in the same way at high temperatures [48]. For $O(n)$ systems [49] (any n), we have,

$$G^{-1}(T, k) = 1 + v(k)/k_B T + O(1/T^3). \quad (36)$$

It is valid to extrapolate this high temperature result to a crossover temperature T_* , if there is no phase transition above T_* and for all relevant real k 's, $|v(k)| \ll k_B T_*$ (an example situation is presented in Sec. VE). Eq. (36) is analytically continued for complex k 's and we have near T_* ,

$$\delta k \sim \left[\frac{m! k_B (T_* - T)}{v^{(m)}(k_*)} \right]^{\frac{1}{m}}, \quad (37)$$

where k_* is a characteristic wave-vector at T_* , δk is how much it changes when the temperature is changed to T (near T_*) and m is the order of the lowest non-vanishing derivative of $v(k)$ at k_* . By our earlier argument, $v'(k_*) = 0$ and $m \geq 2$. In most cases, $m = 2$ and $\nu_L = 1/2$ as before.

We will present below some examples in which our results will be realized.

C. Large n Coulomb frustrated ferromagnet – modulation length exponent at the crossover temperature T_*

Here, and in the next two sub-sections, we discuss the large n limit in $O(n)$ systems. The results in the previous two sections pertain to arbitrary n . We will present here how our result applies to the large n [49] Coulomb frustrated ferromagnet. As is well known [50], in the large n limit, $O(n)$ systems are exactly solvable and behaves as the spherical model [51]. The correlation function in k -space is given by

$$G^{-1}(T, k) = [v(k) + \mu(T)]/k_B T, \quad (38)$$

where $v(k)$ is the Fourier space interaction kernel and $\mu(T)$ is a Lagrange multiplier that enforces the spherical constraint. The paramagnetic transition temperature T_C is obtained from the relation, $\mu(T_C) = -\min_{k \in \mathbb{R}} v(k)$. Below T_C , the Lagrange multiplier $\mu(T) = \mu(T_C)$. Above T_C , $\mu(T)$ is determined from the requirement that $G(\vec{x} = 0) = \frac{1}{N} \sum_{\vec{k}} G(\vec{k}) = 1$. This also implies that, above T_C , small changes in temperature result in proportional changes in $\mu(T)$ and at high temperatures, $\mu(T)$ is a monotonic increasing function of T . The Fourier space interaction $v(k)$ for the Coulomb frustrated ferromagnet is given by $v(k) = Jk^2 + Q/k^2$, where J and Q are positive

constants. The critical temperature, T_C of this system is given by $\mu(T_C) = -2\sqrt{JQ}$. At T_C , the correlation length is infinity and the modulation length is $L_D = 2\pi\sqrt[4]{J/Q}$. As the temperature is increased, the modulation length increases and the correlation length decreases. At T_* , given by $\mu(T_*) = 2\sqrt{JQ}$, the modulation length diverges and the correlation length becomes $\xi = \sqrt[4]{J/Q}$. Above T_* , the correlation function exhibits no modulations and there is one decreasing correlation length and one increasing correlation length. The term in the correlation function with the increasing correlation length becomes irrelevant at high temperatures because of an algebraically decaying prefactor. The divergence of the modulation length at T_* shows an exponent of $\nu_L = 1/2$. [41]

D. An example with $\nu_L \neq 1/2$

Here, we present an example to demonstrate that the exponent for the divergence of the modulation length (and also the correlation length) can be different from $1/2$ in certain special cases. Imagine a large n system for which,

$$v(k) = A(k^2 + l_s^{-2})^2 + 4B(k^2 + l_s^{-2}) + 4C/(k^2 + l_s^{-2}) + D/(k^2 + l_s^{-2})^2, \quad (39)$$

where l_s is a screening length. Adjusting the coupling constants, we find that for $A = B = C = D = 1$, we have a system which has $\nu_L \neq 1/2$ at a crossover temperature. It has a critical temperature T_C , given by $\mu(T_C) = -10$. At T_C , the modulation length is $L_D = 2\pi/\sqrt{1 - 1/l_s^2}$ and the correlation length blows up (as required by definition). We have a crossover temperature T_* given by $\mu(T_*) = 6$. At T_* , the modulation length diverges and the correlation length, $\xi = 1/\sqrt{1 + 1/l_s^2}$. Also, just below T_* , the modulation length L_D diverges as $L_D \propto (T_* - T)^{-1/4}$ meaning that $\nu_L = 1/4$. This is because the first three derivatives of $v(k)$ vanish at $k = i$, which is the characteristic wave-vector at T_* (see Fig. 4).

E. An example in which T_* is a high temperature

Here, we will provide an example of a situation in which the high temperature result of Sec. VB can be applied at a crossover point. Consider the large n system in Eq. (39) with $A = 1$, $B \gg 1$, $C = 1/4$, $D = 0$ and the screening length, $l_s \gg B$. The critical temperature of this system is given by $\mu(T_C) \sim -4\sqrt{B}$ where the modulation length is $L_D \sim 2\pi\sqrt[4]{4B}$. There is a crossover temperature T_* such that $\mu(T_*) \sim 4B^2$. One of the modulation lengths diverges at T_* . The corresponding correlation length is given by $\xi \sim 1/\sqrt{2B}$. This provides an example in which $|v(k)| \ll k_B T_*$ for all real k 's satisfying $|k| \leq \pi$. The second derivative of $v(k)$ is non-zero at the crossover point, resulting in a crossover exponent $\nu_L = 1/2$.

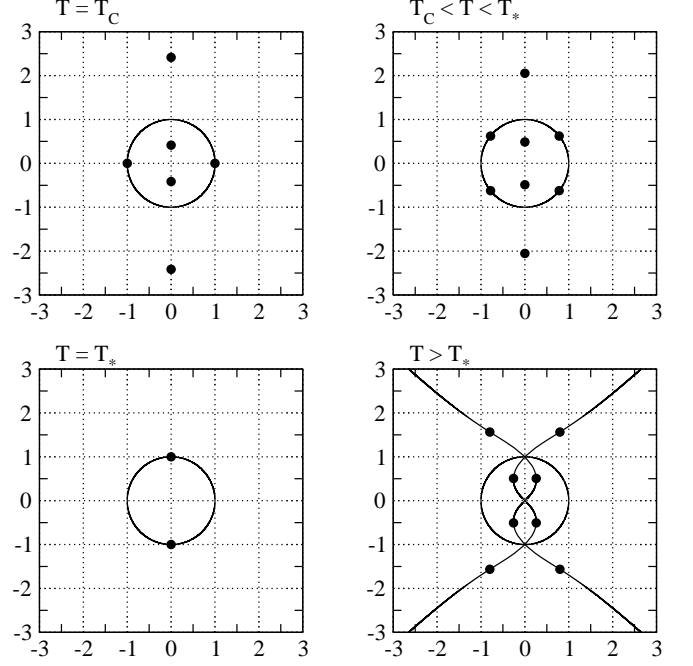


FIG. 4: Location of the poles of the correlation function of the system in Eq. (39) for large l_s (small screening) in the complex k -plane.

VI. CROSSOVERS IN THE ANNNI MODEL

Here we comment on one of the oldest studied examples of a system with a crossover temperature. The following Hamiltonian represents the ANNNI model [36, 37, 43].

$$H = -J_1 \sum_{\langle \vec{x}, \vec{y} \rangle} S(\vec{x})S(\vec{y}) + J_2 \sum_{\langle\langle \vec{x}, \vec{y} \rangle\rangle} S(\vec{x})S(\vec{y}), \quad (40)$$

where as throughout, \vec{x} is a lattice site on a cubic lattice, and the spins $S(\vec{x}) = \pm 1$. The couplings, $J_1, J_2 > 0$. In the summand, $\langle \cdot \rangle$ represents nearest neighbors and $\langle\langle \cdot \rangle\rangle$ represents next nearest neighbors along one axis (say the Z -axis), see Fig. 5(a). Depending on the relative strengths of J_1 and J_2 , the ground state may be either ferromagnetic or in the “ $\langle 2 \rangle$ phase”. The “ $\langle 2 \rangle$ phase”, is a periodic layered phase, in which there are layers of width two lattice constants of “up” spins alternating with layers of “down” spins of the same width, along the Z -axis. As the temperature is increased, the correlation function exhibits jumps in the modulation wave-vector at different temperatures. At these temperatures, the system undergoes first order transitions to different commensurate phases. The inverse correlation function $G^{-1}(T, k)$ is therefore not an analytic function of k and T at the transition points. However, apart from these first order transitions, the phase diagram for the ANNNI model also has several crossovers where the system goes from a

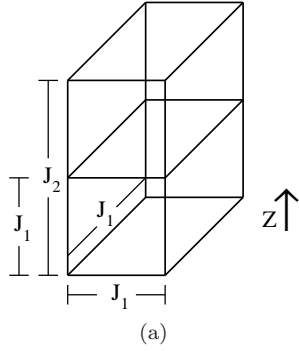


FIG. 5: The coupling constants in the three-dimensional ANNNI model.

commensurate phase to an incommensurate phase with a continuously varying modulation length (see Fig. 6). [52, 53] At these crossover points, following our rigorous analysis, we expect a crossover exponent $\nu_L = 1/2$. Such a scaling of the modulation length has been estimated by several approximate techniques near the “Lifshitz point” P_L . [43, 54–59] The Lifshitz point is the point in the phase diagram of the ANNNI model at which the high temperature paramagnetic phase coexists with the ferromagnetic phase as well as a phase with continuously varying modulation lengths. It is marked as P_L in Fig. 6(b). Although the point P_L has a first order transition, it can be thought of as a limit in which the incommensurate and commensurate regions in Fig. 6(a) shrink and merge to a single point. We would also like to point out that it is known [60] that if the wave-vector takes all possible rational values (“complete devil’s staircase”), we have no first order transitions. Additionally, non-analyticity of the correlation function does not prohibit other quantities from having continuous crossover behavior. For example, the correlation of the fluctuations, i.e., the connected correlation function may generally exhibit continuous variation from a fixed to a variable modulation length phase. If the inverse connected correlation function is analytic, our result can be applied to it resulting in a crossover exponent of $1/2$.

VII. PARAMETER EXTENSIONS AND GENERALIZATIONS

It is illuminating to consider simple generalizations of our result to other arenas. We may also replicate the above derivation for a system in which, instead of temperature, some applied other field λ is responsible for the changes in the correlation function of the system. Some examples could be pressure, applied magnetic field and so on. The complex wave-vector k could also be replaced by a frequency ω whose imaginary part would then correspond to some decay constant in the time domain.

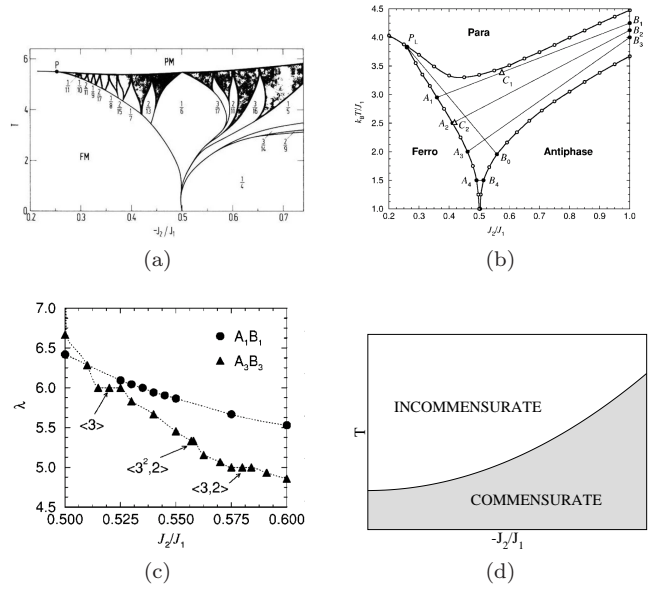


FIG. 6: Existence of incommensurate phases between the commensurate regions in the phase diagram of the ANNNI model. (a) Mean field phase diagram of the ANNNI model in three dimensions. The shaded regions show higher order commensurate phases which have variable modulation length incommensurate phases in between (From Ref. [52]. Reprinted with permission from APS.) (b) Phase diagram for the three-dimensional ANNNI model using a modified tensor product variational approach (From Ref. [53]. Reprinted with permission from APS.) (c) Variation of wavelength along paths A_1B_1 and A_3B_3 of (b) showing a smooth variation of the wavelength near the paramagnetic transition line (From Ref. [53]. Reprinted with permission from APS.) (d) Cartoon of an incommensurate-commensurate crossover region from (a).

More generally, we look for solutions to the equation

$$G^{-1}(\lambda, u) = 0, \quad (41)$$

with the variable u being a variable Cartesian component of the wave-vector, the frequency, or any other momentum space coordinate appearing in the correlation function between two fields ($u = k_i, \omega$, and so on). Replicating our steps mutatis mutandis, we find that the zeros of Eq. (41) scale as $|u - u_0| \propto |\lambda - \lambda_*|^{1/2}$ whenever the real (or imaginary) part of some root becomes constant as λ crosses λ_* . Thus, our predicted exponent of $\nu_L = 1/2$ could be observed in a vast variety of systems in which a crossover occurs as the applied field crosses a particular value, in the complex wave-vector like variable.

Another generalization of our result proceeds as follows [61]. Suppose we have a general *analytic* operator (including any inverse propagator) $G^{-1}(\lambda)$ that depends on a parameter λ . Let a_α be a particular eigenvalue,

$$G^{-1}(\lambda) |a_\alpha(\lambda)\rangle = a_\alpha(\lambda) |a_\alpha(\lambda)\rangle. \quad (42)$$

If $a_\alpha(\lambda)$ changes from being purely real to becoming complex as we change the parameter λ beyond a particular

value λ_* (i.e., $a_\alpha(\lambda > \lambda_*)$ is real and $a_\alpha(\lambda < \lambda_*)$ is complex, or the vice versa), then the imaginary part of $a_\alpha(\lambda)$ will scale (for $\lambda < \lambda_*$ in the first case noted above and for $\lambda > \lambda_*$ in the second one) as $\text{Im} \{a_\alpha(\lambda)\} \propto |\lambda - \lambda_*|^{1/2}$. Similarly, if $a_\alpha(\lambda)$ changes from being pure imaginary to complex at $\lambda = \lambda_*$, then the real part of the eigenvalue will scale in the same way. That is, in the latter instance, $\text{Re} \{a_\alpha(\lambda)\} \propto |\lambda - \lambda_*|^{1/2}$.

In Appendix A, we discuss exponents associated with lock-ins of correlation and modulation lengths in Fermi systems. When dealing with zero temperature behavior, we use the chemical potential μ as the control parameter λ . We discuss metal-insulator transition, exponents in Dirac systems and topological insulators. Additionally, we comment on crossovers related to changes in the Fermi surface topology as well as those related to situations with divergent effective mass.

VIII. IMPLICATIONS FOR THE TIME DOMAIN AND JOSEPHSON TIME-SCALES

The results derived above pertaining to length scales can also be applied to time-scales in which case we look at a temporal correlation function characterized by decay times (corresponding to correlation lengths) and oscillation periods (corresponding to modulation lengths). We may obtain decay time and oscillation period exponents whenever one of these time-scales freezes to a constant value as some parameter λ crosses a threshold value λ_* .

Apart from that, many other phenomena observed with respect to length scales may correspond to similar phenomena in the temporal regime. For instance, in many systems [with correlation functions similar to Eq. (28)], just below the critical temperature, the correlation function as a function of wave-vector, k behaves as

$$G(k) \propto \begin{cases} k^{-2+\eta} & \text{for } k \gg 1/\xi_J, \\ k^{-2} & \text{for } k \ll 1/\xi_J, \end{cases} \quad (43)$$

thus defining the Josephson length-scale, ξ_J [62]. Such an argument could be extended to a time-scale, τ_J (real or imaginary) in systems with Lorentz invariant propagators. For a given wave-vector k , τ_J may be defined as,

$$G(k, \omega) \propto \begin{cases} \omega^{-2+\eta_t} & \text{for } \omega \gg 1/\tau_J, \\ \omega^{-2} & \text{for } \omega \ll 1/\tau_J, \end{cases} \quad (44)$$

where ω is the frequency conjugate to time while performing the Fourier transform and $\eta_t (\neq 0)$ is an anomalous exponent for the time variable.

IX. CHAOS AND GLASSINESS

So far in this work, we have considered phases in which the modulation length is well defined. For completeness, in this section, we mention situations in which aperiodic phases may be observed. Such phenomena are

well known [60, 63]. The basic idea is as follows. It is known that nonlinear dynamical systems may have solutions that exhibit chaos. If the configuration of a system is governed by an equation which takes the form of a nonlinear dynamical system when a spatial coordinate (x) is replaced by time (t), we may observe spatial chaos as a function of that coordinate. Such configurations may naturally correspond to amorphous systems and realize models of structural glasses. Such a correspondence has been discussed in the realm of spin glasses, wherein spin glass transitions in random Potts systems and hard computational problems coincide with transitions from ordered to chaotic phases in derived mechanical systems.[64]

The free energy of our system in the continuum is given by

$$\mathcal{F}[s] = \frac{1}{2} \int \frac{d^d k}{(2\pi)^d} (v(\vec{k}) + \mu) |s(\vec{k})|^2. \quad (45)$$

Adding a quartic interaction, like in Eq. (4), we have,

$$\mathcal{F}[s] = \frac{1}{2} \int \frac{d^d k}{(2\pi)^d} (v(\vec{k}) + \mu) |s(\vec{k})|^2 + \frac{u}{4} \int d^d x (S^2(\vec{x}) - 1)^2. \quad (46)$$

This corresponds to an Ising system in the limit of large u , wherein $S^2(\vec{x}) = 1$ is strictly enforced. For finite or small u , this free energy corresponds to a “soft-spin” model in which $S(\vec{x})$ is not exactly normalized.

The Euler-Lagrange equation for the spins $S(\vec{x})$ obtained by extremizing the free energy of Eq. (46) often takes the form of non-linear differential equations (as discussed in Appendix B). Non-linear dynamical systems may exhibit chaotic behavior. In general, a dynamical system may, in the long time limit, either veer towards a fixed point, a limit cycle, or exhibit chaotic behavior. We should therefore expect to see such behavior in the spatial variables in systems which are governed by Euler-Lagrange equations with forms similar to nonlinear dynamical systems. Upon formally replacing the temporal coordinate by a spatial coordinate, chaotic dynamics in the temporal regime map onto to a spatial amorphous (glassy) structure.

For example, the simple system with dispersion $v(k)$ in Eq. (46) given by

$$v(k) = k^4 - c_1 k^2 + c_2, \quad (47)$$

where c_1 and c_2 are constants may give rise to glassy structures for non zero u . Such a dispersion may arise in the continuum limit of hypercubic lattice systems with range four interactions (giving rise to the k^4 term) and nearest neighbor interactions (giving rise to the k^2 term). In Fig. 7(a), we illustrate the spatial amorphous glass-like chaotic behavior that this system exhibits. In Figs. 7(b)–7(g), we provide plots of the spatial derivatives of different order vs each other (and $S(x)$ itself).

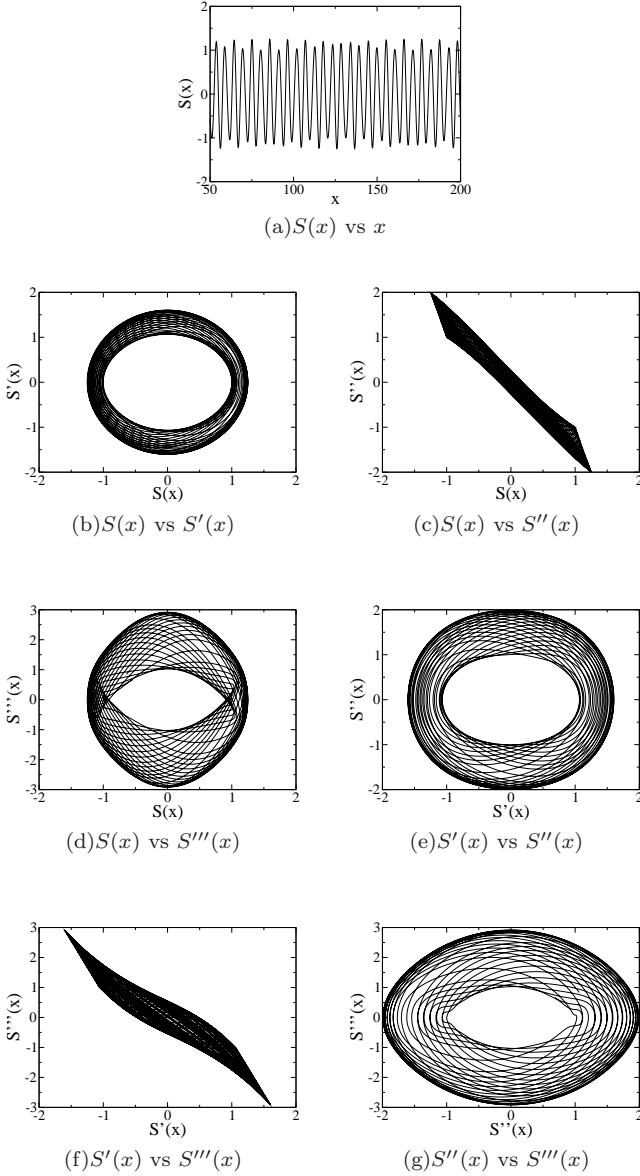


FIG. 7: Glassiness in system with $v(k)$ as in Eq. (47) with $c_1 = 5$, $c_2 = 4$ and $u = 1$ and $\mu = 1$ in Eq. (46).

Another example comes from the spatial analog of dynamical systems with nonlinear “jerks”. It is well known that systems with nonlinear “jerks” often give rise to chaos [65]. “Jerk” here refers to the time derivative of a force, or, something which results in a change in the acceleration of a body. Translating this idea from the temporal regime to the spatial regime, one can expect to obtain a aperiodic/glassy structure in a system for which the Euler Lagrange equation, Eq. (B1) may seem simple. For example, if we have the following, Euler Lagrange equation for a particular one-dimensional system,

$$S'''(x) = J(S(x), S'(x), S''(x)) \quad (48)$$

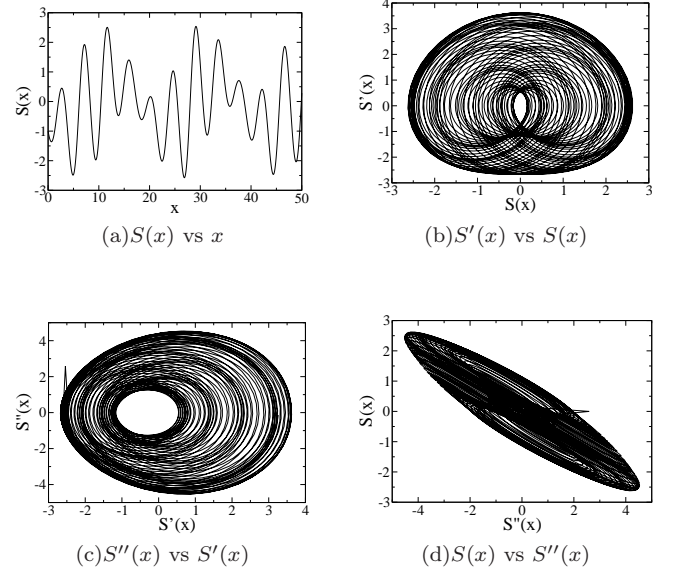


FIG. 8: Example of aperiodic structure inspired by system with nonlinear jerks. Here $J(S(x), S'(x), S''(x)) = -2S'(x) + (|S(x)| - 1)$ and initial conditions are $S(0) = -1$, $S'(0) = -1$, $S''(0) = 1$ (chosen from Ref. [65]).

where $J(S(x), S'(x), S''(x))$ has a nonlinear term, then the system may have aperiodic structure. An example is shown in Fig. (8).

We now discuss $O(n)$ systems and illustrate that the existence of periodic solutions (and absence of chaos) in a broad class of systems.

The Euler-Lagrange equations in Eqs. (B1, B7) become linear in case of “hard” spins, i.e., when the $O(n)$ condition is strictly enforced, i.e., $u \rightarrow \infty$. In this case, all configurations in the system can be described by a finite set of modulation wave-vectors (as was the case for the ground states in Sec. V A).

There are two ways to obtain this result. The first one is by arguing that since the Euler-Lagrange equations represent a *finite* set of coupled *linear* ordinary differential equations, chaotic solutions are not present. The configurations, therefore must be characterized by a finite number of modulation wave-vectors.

The second approach is more quantitative. The idea used here is the same as the one used in Ref. [47]. An identical construct can be applied to illustrate that spiral/poly-spiral states are the only possible states that satisfy the Euler-Lagrange equation if $n > 1$. We write the Euler-Lagrange equations in Fourier space.

$$D(\Delta_{\vec{k}})s(\vec{k}) = 0. \quad (49)$$

We obtain a set of wave-vectors, $\mathcal{K} = \{\vec{q}_m\}$ that satisfy Eq. (49). We assume that in the Fourier space the Euler-

Lagrange equations have real wave-vectors as solutions.

$$D(\Delta_{\vec{k}})s(\vec{k})\Big|_{\vec{k}=\vec{q}_m} = 0. \quad (50)$$

To obtain an upper limit on the number of wave-vectors that can be used to describe a general configuration satisfying the Euler-Lagrange equations, we assume that: **(i)** $2(\vec{q}_m \pm \vec{q}_{m'}) \neq k_R$ for any $\vec{q}_m, \vec{q}_{m'} \in \mathcal{K}$, where k_R represents a reciprocal lattice vector; and, **(ii)** $\vec{q}_m \pm \vec{q}_{m'} \neq \vec{q}_p \pm \vec{q}_{p'}$ for any $\vec{q}_m, \vec{q}_{m'}, \vec{q}_p, \vec{q}_{p'} \in \mathcal{K}$. Let a particular state be described as

$$\vec{S}_0(\vec{x}) = \sum_m \vec{a}_m e^{-i\vec{q}_m \cdot \vec{x}}, \quad (51)$$

where the vectors \vec{a}_m have n components for $O(n)$ systems. Since the states must have real components, the above equation must take the form,

$$\vec{S}_0(\vec{x}) = \sum_{m=1}^{N_q} (\vec{a}_m e^{-i\vec{q}_m \cdot \vec{x}} + \vec{a}_m^* e^{i\vec{q}_m \cdot \vec{x}}), \quad (52)$$

where \vec{a}_m^* is the vector whose components are complex conjugates of the vector \vec{a}_m . In Eq. (52), we do not count terms involving the wave-vectors \vec{q}_m and $-\vec{q}_m$ separately as such terms has been explicitly written in the sum.

We define the complex vectors $\{|U_m\rangle\}$ and $\{|V_m\rangle\}$ as,

$$\begin{aligned} |U_m\rangle &= \vec{a}_m e^{-i\vec{q}_m \cdot \vec{x}}, \\ |V_m\rangle &= \vec{a}_m e^{i\vec{q}_m \cdot \vec{x}}. \end{aligned} \quad (53)$$

The $O(n)$ normalization condition can then be expressed as,

$$\begin{aligned} \sum_m \langle U_m | U_m \rangle &= n, \\ \sum_m \langle V_m | V_m \rangle &= n, \\ \sum_{\vec{q}_m - \vec{q}_{m'} = \vec{A}} (\langle U_m | U_{m'} \rangle + \langle V_{m'} | V_m \rangle) + \\ \sum_{\vec{q}_m + \vec{q}_{m'} = \vec{A}} (\langle U_m | V_{m'} \rangle + \langle U_{m'} | V_m \rangle) &= 0. \end{aligned} \quad (54)$$

Solutions to Eq. (54) are spanned by the set of basis vectors $\{|U_m\rangle\}$ and $\{|V_m\rangle\}$.

$$\begin{aligned} \langle U_m | U_{m'} \rangle &= \delta_{m,m'}, \\ \langle U_m | V_{m'} \rangle &= 0, \\ \langle V_m | V_{m'} \rangle &= \delta_{m,m'}, \end{aligned} \quad (55)$$

These would require a minimal vector space which has $2N_q$ dimensions for description. Since these vectors are described by n -components, we require,

$$N_q \leq n/2. \quad (56)$$

Therefore, the states satisfying the Euler-Lagrange equations for an $O(n \geq 2)$ system can at most be characterized by $n/2$ pairs of wave-vectors. These states can be

described by N_q spirals each described in a plane formed by a pair of $O(n)$ directions. Such states are therefore called poly-spiral states.

The bound presented in this result is stronger than the one obtained by simple balancing of the number of constraints with the number of degrees of freedom [66].

A few remarks are in order.

- When u in Eq. (46) is finite, i.e., in the soft spin regime, poly-spiral solutions could be present even though aperiodic solutions are also allowed.
- *Continuum limit:* In the hard-spin limit, i.e., $u \rightarrow \infty$ in Eq. (46), if the Fourier space Euler-Lagrange equation is satisfied by non-zero real wave-vectors, we have poly-spiral solutions as in the lattice case. When u is finite, aperiodic solutions may also be present.
- If the Fourier space Euler-Lagrange equation does not have any real wave-vector solution, poly-spiral states are not observed.

In nonlinear dynamical systems, chaos is often observed via *intermittent phases*. As a tuning parameter λ is varied, the system enters a phase in which it jumps between periodic and aperiodic phases until the length of the aperiodic phase diverges. This divergence is characterized by an exponent $\nu = 1/2$ similar to ours.[67]

X. CONCLUSIONS

Most of the work concerning properties of the correlation functions in diverse arenas, has to date focused on the correlation lengths and their behavior. In this work, we examined the oscillatory character of the correlation functions when they appear.

We furthermore discussed when viable non-oscillatory spatially chaotic patterns may (or may not appear); in these, neither uniform nor oscillatory behavior is found. Our results are universal and may have many realizations. Below, we provide a brief synopsis of our central results.

1. We have shown the existence of a universal modulation length exponent $\nu_L = 1/2$ [Eq. (16)]. Here the scaling could be as a function of some general parameter λ such as temperature. This is observed in systems with analytic crossovers including the commensurate-incommensurate crossover in the ANNNI model.
2. In certain situations the above exponent could take other rational values [Eq. 14].
3. This result also applies to situations where a correlation length may lock in to a constant value as the parameter λ is varied across a threshold value [as in Eq. (23)].

4. We extended our result to include situations in which the crossover might take place at a branch point. In this case irrational exponents could also be present. In Eqs. (31, 32), we provide universal scaling relations for correlation and modulation lengths.
5. We illustrate that discontinuous jumps in the modulation/correlation lengths mandate a thermodynamic phase transition.
6. Our results apply to both length scales as well as time-scales. We further introduce the notion of a Josephson time-scale.
7. We comment on the presence of aperiodic modulations/amorphous states in systems governed by nonlinear Euler-Lagrange equations. We illustrate that in a broad class of multi-component systems chaotic phases do not arise. Spiral/poly-spiral solutions appear instead.
8. Our results have numerous applications. We discussed several non-trivial consequences for classical system in the text. For completeness, in Appendix A, we discuss, rather simple applications of our results to non-interacting Fermi systems. We mention situations in which the Fermi surface changes topology, situations with divergent effective masses and the metal-insulator transition. We further discuss applications to many other systems including Dirac systems and topological insulators. Aside from uniform and regular modulated periodic states of various strongly correlated electronic systems [2–10], there are numerous suggestions and indications of glassy (and spatially non-uniform or chaotic) behavior that naturally lead to high entropy in these systems, e.g., [68–71]. In future work, we will elaborate on non-trivial consequences of our results for interacting Fermi systems.

Finally, we make a brief parenthetic remark concerning the “fractal dimension” in glasses and other systems. The notion of fractal dimensionality was recently applied in Ref. [72] based on a comparison between the atomic volume and the reciprocal of the dominant peak K_R in the structure factor in metallic glasses. Specifically, the volume $V \sim K_R^{-D_f}$ with D_f being the fractal dimension. This definition is very intuitive and such a relation between volume and structure factor peaks is to be expected for a system of dimension D_f is all natural scales in the parameter expand or contract with temperature (or other parameters) in unison. However, as we elaborated on at length, aside from global changes in the lattice constant, K_R can change non-trivially with temperature and other parameters in some regular lattice and other systems. Formally, this may give rise to an effective non-trivial fractal dimension in various systems.

Acknowledgments. The work at Washington University in St Louis has been supported by the National

Science Foundation under NSF Grant numbers DMR-1106293 (Z.N.) and DMR-0907793 (A.S.) and by the Center for Materials Innovation. Z.N.’s research at the KITP was supported, in part, by the NSF under Grant No. NSF PHY11-25915. Z.N. is grateful to the inspiring KITP workshops on “Electron glass” and “Emerging concepts in glass physics” in the summer of 2010. V.D. was supported by the NSF through Grant DMR-1005751.

Appendix A: Fermi systems

In this appendix, we consider several examples of fermionic systems where we observe a correlation or modulation length exponent. We discuss low and intermediate temperature length scales, metal-insulator transitions, Dirac systems and topological insulators. For Fermi systems, we have,

$$\langle n(\vec{k}) \rangle = \langle c^\dagger(\vec{k})c(\vec{k}) \rangle = \frac{1}{e^{\beta(\epsilon(\vec{k})-\mu)} + 1}, \quad (\text{A1})$$

where $c(\vec{k})$ and $c^\dagger(\vec{k})$ are the annihilation and creation operators at momentum \vec{k} and $\beta = 1/(k_B T)$ with T the temperature. The hopping amplitude/correlation function across a distance \vec{x} is given by

$$G(\vec{x}) = \langle C^\dagger(0)C(\vec{x}) \rangle = \sum_{\vec{k}} \langle n(\vec{k}) \rangle e^{-i\vec{k} \cdot \vec{x}} \quad (\text{A2})$$

In this section, at several instances, we will consider scaling of correlation and modulation lengths with the chemical potential μ . We will use the letter ν to represent exponents corresponding to scaling with respect to μ and continue to use ν to represent scaling with respect to the temperature T .

1. Zero temperature length scales – Scaling as a function of the chemical potential μ

We consider a fermionic system with energy $\epsilon(\vec{k})$ in Fourier space. At zero temperature, the number of particles having wave-vector \vec{k} is given by

$$\langle n(\vec{k}) \rangle = \begin{cases} 1 & \text{for } \epsilon(\vec{k}) < \mu \\ 0 & \text{for } \epsilon(\vec{k}) > \mu \end{cases} \quad (\text{A3})$$

In this system, the modulation lengths exhibited by the system are governed by the Fermi surface (surface/contour defined by $\epsilon(\vec{k}) = \mu$) and the boundaries of the Brillouin zone (showing the periodicity of the real-space lattice). To get the modulation lengths along some chosen direction, a line along that direction must be drawn and its intersection with the Fermi surface will give the different length scales. If we change μ we effectively change the density, ρ .

$$\rho = \int_{\epsilon(\vec{k}) < \mu} \frac{d^d k}{(2\pi)^d}. \quad (\text{A4})$$

We see the following effects on the characteristic length scales as the *Fermi surface changes topology* at $\mu = \mu_0$ and at $\mu = \mu'_0$ in Fig. 9.

(i) If as we change μ , two branches of the Fermi surface touch each other at $\mu = \mu_0$ and separates again as we go past μ_0 , we get a smooth crossover from one set of modulation lengths to another with $|L_D - L_{D0}| \propto |\mu - \mu_0|$ on both sides of the crossover. This gives us an exponent $v_L = 1$. Examples of this occur at half filling of the square lattice tight binding model and at three-quarters filling of the triangular lattice tight binding model. These will be discussed later.

(ii) If on the other hand, one branch of the Fermi surface vanishes as we go past $\mu = \mu_0$, the crossover is not so smooth and we get some rational fraction v_L (usually $v_L = 1/2$) as the crossover exponent: $|L_D - L_{D0}| \propto |\mu - \mu_0|^{v_L}$, on one side of the crossover. An example of this is shown in Fig. 9. Here,

$$|L_D - L_{D0}| = \frac{L_{D0}^2}{2\pi} \sqrt{\frac{2|\mu - \mu_0|}{|\epsilon''(2\pi/L_{D0})|}}, \quad (\text{A5})$$

where L_{D0} is the modulation length at the point where the $\mu = \mu_0$ line touches the $\epsilon(k)$ curve, such that $\epsilon'(2\pi/L_{D0}) = 0$. The hopping correlation function takes the form,

$$G(x) = \frac{(ax)^{d/2} J_{d/2}(ax)}{(2\pi)^{d/2} x^d} - \frac{(bx)^{d/2} J_{d/2}(bx)}{(2\pi)^{d/2} x^d} + \frac{(cx)^{d/2} J_{d/2}(cx)}{(2\pi)^{d/2} x^d}, \quad (\text{A6})$$

where $\mu'_0 < \mu < \mu_0$ and a, b and c in Eq. (A6) (corresponding to modulation lengths of $2\pi/a, 2\pi/b$ and $2\pi/c$) are the values of k for which $\epsilon(k) = \mu$ (as shown in Fig. 9).

At arbitrarily small but finite temperatures, the correlation length has terms exhibiting modulations of all possible wavelengths. The weights of such terms, however, are suppressed by an exponential prefactor which depends on the difference of $\epsilon(\vec{k})$ from μ for that wave-vector. As an illustrative example see Fig. 10. Apart from the zero temperature term, which only gets contributions from the wave-vector k_2 , we have finite temperature contributions for wave-vectors for which $|\epsilon(k) - \mu|$ is small. Near k_2 , we can assume $\epsilon(k)$ is linear such that $\epsilon(k) \approx \mu + (k - k_2)\epsilon'(k_2)$. Similarly, near k_1 , $\epsilon(k) - \mu \approx -\Delta - (k - k_1)^2 \epsilon''(k_1)/2$, where $\Delta = \mu - \mu_0$ (see Fig. 10). For large β , both these contributions are highly localized around k_2 and k_1 respectively making the above approximations very good and the Fourier transforming integrals easy to evaluate ($\langle n(\vec{k}) \rangle$ taking exponential and Gaussian forms). We have,

$$G(x) = \frac{(k_2 x)^{d/2} J_{d/2}(k_2 x)}{(2\pi)^{d/2} x^d} - \frac{2(k_2 x)^{d/2} J_{d/2-1}(k_2 x)}{(2\pi)^{d/2} \beta \epsilon'(k_2) x^{d-1}} + \frac{e^{-\beta \Delta} (k_1 x)^{d/2} J_{d/2-1}(k_1 x)}{(2\pi)^{\frac{d-1}{2}} \sqrt{\beta \epsilon''(k_1)} x^{d-1}}, \quad (\text{A7})$$

where $\beta \rightarrow \infty$ and $\Delta \rightarrow 0$, such that $\beta \Delta \rightarrow \infty$.

Next, we will discuss scaling of the modulation length in with the chemical potential, μ in the familiar tight binding models on the square and triangular lattices at zero temperature.

a. Tight binding model on the square lattice

We consider a two-dimensional tight binding model of the square lattice. The energy in Fourier space is given by

$$\epsilon(\vec{k}) = -2t (\cos k_x + \cos k_y) \quad (\text{A8})$$

The constant energy contours corresponding to Eq. (A8) are drawn in Fig. 11. As is clear from Fig. 11, there are certain directions (e.g., along the X -axis) along which there is no \vec{k} for $\epsilon(\vec{k}) > 0$. If we consider the same system at zero temperature, the following three crossovers are observed.

(i) *Half filling*: The chemical potential μ is zero at the half filling state. The Fermi surface is given by $\pm k_x \pm k_y = \pi$. For small μ , we have,

$$\pm k_x \pm k_y = \pi + \frac{\mu}{2t \sin k_x}, \quad (\text{A9})$$

thus giving us an uninteresting modulation exponent, $v_L = 1$.

(ii) *Empty band*: When $\mu = -4t$, none of the states are occupied. As we increase μ by a tiny amount $\delta\mu$ above this value, we observe a non-zero modulation wave-vector, $k = \sqrt{\delta\mu}/t$, thus showing a modulation exponent $v_L = 1/2$.

(iii) *Full inert bands*: When $\mu = +4t$, all the states are occupied. As we lower μ by a tiny amount $\delta\mu$ below this value, we observe a difference δk of the modulation vector from $\pm \hat{e}_x \pi \pm \hat{e}_y \pi$. We have, $\delta k = \sqrt{\delta\mu}/t$, thus showing a modulation exponent $v_L = 1/2$ again.

b. Tight binding model on the triangular lattice

The triangular lattice with the tight binding approximation, is very similar to the square lattice. The energy $\epsilon(\vec{k})$ in Fourier space is given by

$$\epsilon(k) = -2t \cos k_x - 4t \cos \frac{k_x}{2} \cos \frac{k_y \sqrt{3}}{2}. \quad (\text{A10})$$

The Fermi surfaces for chemical potentials μ close to three-quarters filling are shown in Fig. 12. We have exponents similar to the square lattice.

(i) *Three-quarters filling*: The chemical potential $\mu = 2t$ corresponds to the three-quarters filling state. If we concentrate on the $\{k_x = \pi, k_y : -\pi/\sqrt{3} \rightarrow \pi/\sqrt{3}\}$ segment (same phenomenon is present at all the other segments

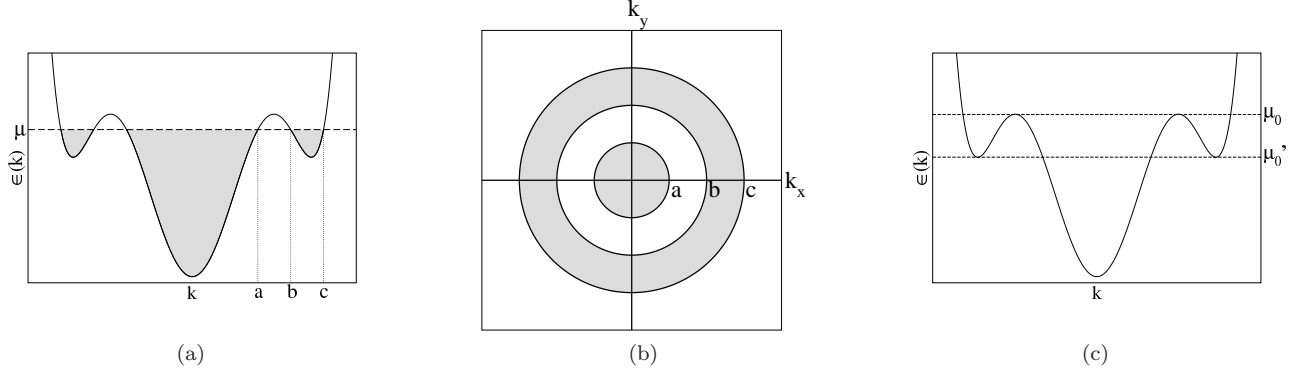


FIG. 9: Example of a Fermi system where the modulation length exponent is $1/2$. The gray region shows the filled states. When $\mu > \mu_0$, modulations corresponding to wave-vectors $k = a$ and $k = b$ cease to exist and we get an exponent of $1/2$ at this crossover. Similarly, when $\mu < \mu'_0$, modulations corresponding to wave-vectors $k = b$ and $k = c$ die down.

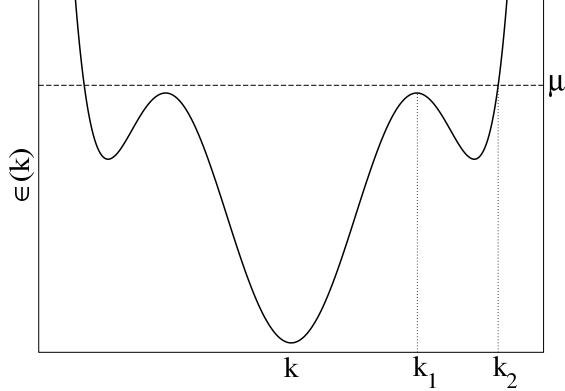


FIG. 10: The same Fermi system as in Fig. 9, but now with a chemical potential $\mu = \mu_0 + \Delta$, slightly higher than μ_0 . The temperature is small but finite.

of the quarter filling Fermi surface), we get,

$$\delta k_x \sim \frac{\delta \mu}{2 \cos\left(\frac{k_y \sqrt{3}}{2}\right)}, \quad (\text{A11})$$

where $k_x = \pi + \delta k_x$ is obtained when $\mu = 2t + \delta \mu$. This gives us a modulation exponent, $v_L = 1$.

(ii) *Empty band:* When $\mu = -6t$, none of the states is occupied. As we increase μ by a tiny amount $\delta \mu$ above this value, we observe a non-zero modulation wave-vector, $k = \sqrt{2\delta \mu/3}$, thus showing a modulation exponent $v_L = 1/2$.

(iii) *Full inert bands:* When $\mu = 3t$, all of the states are occupied and close to this value the Fermi surface is composed of six small circles around $\vec{k} = \hat{x} \cos(n\pi/3) +$

$\hat{y} \sin(n\pi/3)$, $n = \{0, 1, 2, 3, 4, 5\}$. If $\mu = 3t - \delta \mu$, we get, $|\delta \vec{k}| = 2\sqrt{\delta \mu/3}$, again giving us a modulation length exponent, $v_L = 1/2$.

c. Metal-Insulator transition

We apply our result to metal to band insulator transitions at zero temperature. This happens when the Fermi

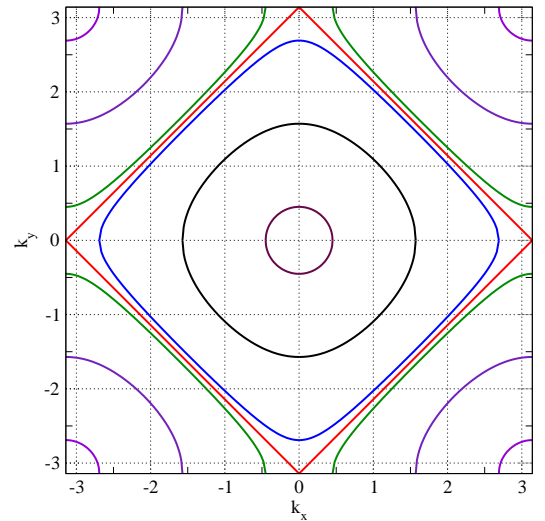


FIG. 11: Constant energy contours for two-dimensional tight binding model on the square lattice in Eq. (A8). The red square corresponds to the particle hole symmetric contour where $\epsilon(\vec{k}) = 0$. The contours inside it are for negative $\epsilon(\vec{k})$ and those outside are for positive $\epsilon(\vec{k})$.

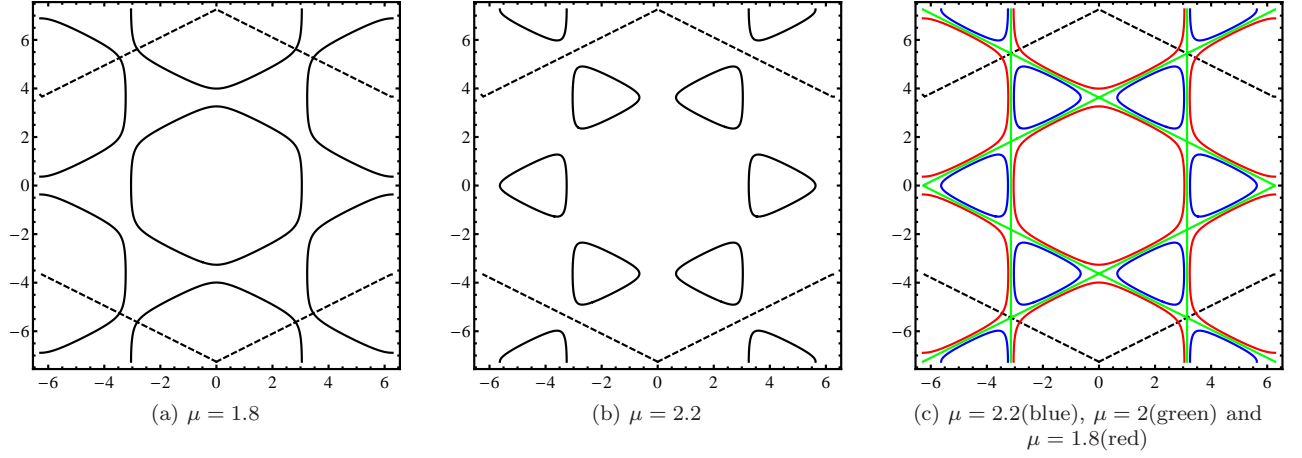


FIG. 12: Fermi surface for a triangular lattice with tight binding. The dashed lines are the Brillouin zone boundaries. This demonstrates a smooth crossover from one set of Fermi surface branches to another as μ is changed across $\mu = 2$. The points where the crossovers take place are $(0, \pm 2\pi/\sqrt{3})$, $(\pm\pi, \pm\pi/\sqrt{3})$. The modulation length exponent for this crossover is $v_L = 1$.

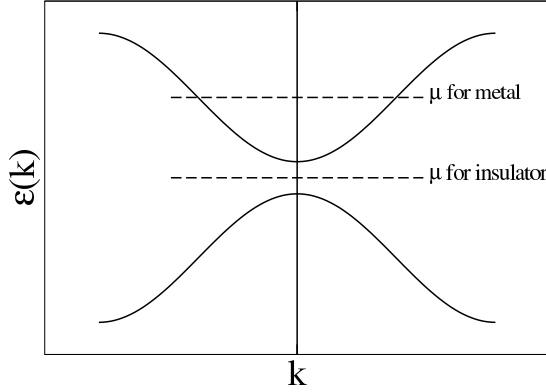


FIG. 13: Illustration of a transition from a metal to a band insulator. This figure is for illustration only.

energy is changed such that all occupied bands are completely full, i.e., there is no partially filled band (as in Fig. 13). In the insulator, the Fermi energy lies in between two bands and thus the filled states are separated from the empty states by a finite energy gap. As the Fermi energy is tuned, the Fermi energy might touch one of the bands thereby rendering the system metallic. Close to this transition the energy is quadratic in the momentum k , i.e., $|k| \propto |\delta\mu|^{1/2}$. This implies that,

$$|\delta k| \propto |\delta\mu|^{1/2} \quad (\text{A12})$$

Following Eq. (16), $v_L = 1/2$. As usual, the exponent v_L characterizes changes in the chemical potential μ which lead to deviations of the modulation length from

the value which appears at the point where the system turns metallic from the insulating regime.

d. Dirac systems

The low energy physics of graphene and Dirac systems in general is characterized by the existence of Dirac points in momentum space where the density of states vanishes and the energy, $\epsilon(k)$ is proportional to the momentum k for small k . In such systems, when we apply our routine we observe an exponent,

$$\begin{aligned} |\delta k| &\propto |\delta\mu| \\ \Rightarrow v_{Dirac} &= 1 \end{aligned} \quad (\text{A13})$$

whenever a length-scale diverges.

e. Topological Insulators – Multiple length-scale exponents as a function of the chemical potential μ

An interesting application of our results to topological insulators adds a new interesting facet to these already fascinating systems. The low energy physics of some three-dimensional topological insulators can be obtained from the following effective Hamiltonian[73] in momentum space.

$$H(\vec{k}) = \epsilon_0(\vec{k})I_{4 \times 4} + \begin{pmatrix} \mathcal{M}(\vec{k}) & A_1 k_z & 0 & A_2 k_- \\ A_1 k_z & -\mathcal{M}(\vec{k}) & A_2 k_- & 0 \\ 0 & A_2 k_+ & \mathcal{M}(\vec{k}) & -A_1 k_z \\ A_2 k_+ & 0 & -A_1 k_z & -\mathcal{M}(\vec{k}) \end{pmatrix} \quad (\text{A14})$$

where $\epsilon_0(\vec{k}) = C + D_1 k_z^2 + D_2 k_\perp^2$, $\mathcal{M}(\vec{k}) = M - B_1 k_z^2 - B_2 k_\perp^2$, with $k_\pm = k_x + ik_y$, $k_\perp = \sqrt{k_x^2 + k_y^2}$ and A_1, A_2 ,

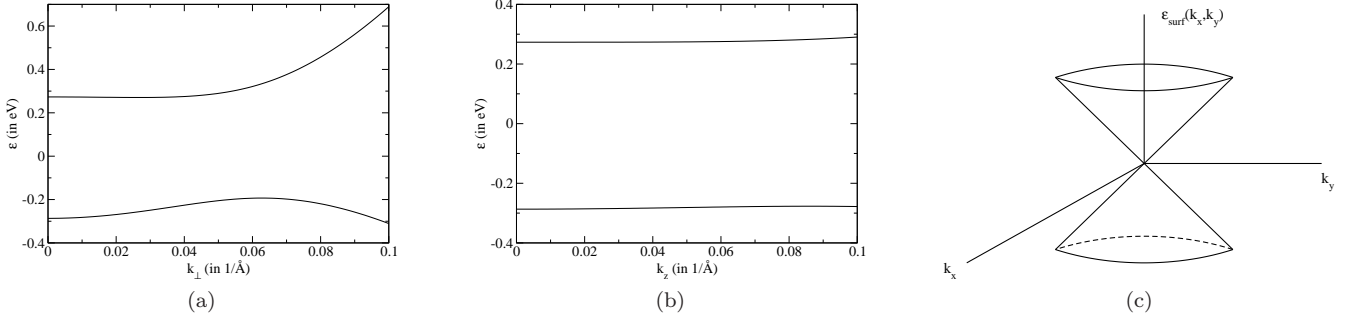


FIG. 14: Energy levels of Bi_2Se_3 topological insulator.

14(a): $\epsilon(\vec{k})$ versus k_{\perp} at $k_z = 0$; 14(b): $\epsilon(\vec{k})$ versus k_z at $k_{\perp} = 0$; 14(c): $\epsilon_{surf}(k_x, k_y)$ versus $k_{\perp} \equiv (k_x, k_y)$.

B_1, B_2, C, D_1 and D_2 constants for a given system. This corresponds to energy levels given by

$$\epsilon(\vec{k}) = \epsilon_0(\vec{k}) \pm \sqrt{\mathcal{M}(\vec{k})^2 + A_1 k_z^2 + A_2 k_{\perp}^2} \quad (A15)$$

This is plotted in Figs. 14(a) and 14(b). The finite gap between the two bands results in exponentially damped hopping amplitude, characterized by a finite correlation length when the Fermi energy lies within this gap. These energy bands vary quadratically for small k this giving

$$\begin{aligned} |\delta k| &\propto \sqrt{|\delta \mu|} \\ \Rightarrow v_{bulk} &= 1/2 \end{aligned} \quad (A16)$$

whenever the correlation length diverges and a insulator to metal transition takes place in the bulk, thus allowing long range hopping. The same exponent is also expected whenever the modulation length becomes constant as μ crosses some threshold value. The surface states on the other hand are not always so smooth. For the same systems as above the effective Hamiltonian for the surface states is

$$H_{surf} = \begin{pmatrix} 0 & A_2 k_{-} \\ A_2 k_{+} & 0 \end{pmatrix} \quad (A17)$$

The surface energy levels are given by

$$\epsilon_{surf}(k_x, k_y) = \pm A_2 k_{\perp}. \quad (A18)$$

Thus the energy profile at the surface is like Fig. 14(c). Just like the Dirac points in graphene, we observe an exponent

$$v_{surf} = 1. \quad (A19)$$

f. An example of a zero temperature Fermi system in which v_L is not half or one

Very large (or divergent) effective electronic masses m_{eff} can be found in heavy fermion systems (and at putative quantum critical points). [74, 75] If the electronic

dispersion $\epsilon(\vec{k})$ has a minimum at \vec{k}_0 then a Taylor expansion about that minimum will read

$$\begin{aligned} \epsilon(\vec{k}) &= \epsilon(\vec{k}_0) + \frac{\hbar^2}{2} \sum_{ij} (m_{eff}^{-1})_{ij} (k_i - k_{0i})(k_j - k_{0j}) + \\ &\sum_{ijl} A_{ijl} (k_i - k_{0i})(k_j - k_{0j})(k_l - k_{0l}) + \dots \end{aligned} \quad (A20)$$

When present, parity relative to \vec{k}_0 or other considerations may limit this expansion to contain only even terms. As an example, we consider the dispersion

$$\epsilon(k) = c_1 - c_2(k^2 - k_0^2)^4, \quad (A21)$$

where $c_2 > 0$. The hopping correlation function of such a system has a term which exhibits modulations at wave-vector $k = k_0$ at $\mu = \mu_* = c_1$. At higher values of the chemical potential, such a term ceases to exist. At lower values ($\mu = \mu_* - \delta\mu$), this term breaks up into two terms whose modulation wave-vectors are different from k_0 by,

$$\begin{aligned} k - k_0 &\sim \pm \frac{\delta\mu^{1/4}}{2k_0 c_2^{1/4}}, \\ \Rightarrow v_L &= 1/4. \end{aligned} \quad (A22)$$

2. Finite temperature length scales – Scaling as a function of temperature

At finite temperatures, apart from having the modulation lengths (as for the zero temperature situation), we have, in general, a set of characteristic correlation lengths. From Eq. (A2), these are obtained by finding the poles of the Fermi function. Along some direction \hat{e}_0 , a pole $\vec{k}_0 = \hat{e}_0 k_0$ with $k_0 = \pm 2\pi/L_0 \pm i/\xi_0$. This satisfies,

$$\epsilon(\vec{k}_0) = \mu + (2n + 1)i/\beta, \quad (A23)$$

where n is an integer. For a given μ , let us suppose that as we change the temperature, at $T = T_0$, we reach

a saddle point of $\epsilon(\vec{k})$ in the complex plane of one of the components of \vec{k} . Then, near the saddle point, the corresponding correlation and modulation lengths behave as,

$$\begin{aligned} |L_D - L_{D0}| &\propto |T - T_0|^{\nu_L}, \\ |\xi - \xi_0| &\propto |T - T_0|^{\nu_c}, \end{aligned} \quad (\text{A24})$$

where $\nu_L = \nu_c = 1/2$ in most cases (when the second derivative is not zero).

Appendix B: Euler-Lagrange equations for scalar spin systems

Here, we discuss an alternative approach for analyzing our systems. In this approach, we study the Euler-Lagrange equations for the system corresponding to extremization of the free energy in Eq. (46). The Euler-Lagrange equations take the form,

$$\begin{aligned} \int d^d y \tilde{V}(\vec{x} - \vec{y}) S(\vec{y}) + \mu S(\vec{x}) \\ + u(S^2(\vec{x}) - 1)S(\vec{x}) = 0, \end{aligned} \quad (\text{B1})$$

where $\tilde{V}(\vec{x}) = [V(\vec{x}) + V(-\vec{x})]/2$. For example, if we consider the finite ranged system for which,

$$\begin{aligned} \int d^d y \tilde{V}(\vec{x} - \vec{y}) S(\vec{y}) = a \nabla^2 S(\vec{x}) \\ + b \nabla^4 S(\vec{x}) + \dots, \end{aligned} \quad (\text{B2})$$

we then will have,

$$\begin{aligned} a \nabla^2 S(\vec{x}) + b \nabla^4 S(\vec{x}) + \dots + \mu S(\vec{x}) \\ + u(S^2(\vec{x}) - 1)S(\vec{x}) = 0. \end{aligned} \quad (\text{B3})$$

For lattice systems the Euler Lagrange equation (B1)

takes the form,

$$\begin{aligned} \sum_{\vec{y}} \tilde{V}(\vec{x} - \vec{y}) S(\vec{y}) + \mu S(\vec{x}) \\ + u(S^2(\vec{x}) - 1)S(\vec{x}) = 0. \end{aligned} \quad (\text{B4})$$

In general, it may be convenient to express the linear terms in the above equation in terms of the lattice Laplacian Δ . We write

$$D(\Delta)S(\vec{x}) \equiv \sum_{\vec{y}} \tilde{V}(\vec{x} - \vec{y}) S(\vec{y}) + \mu S(\vec{x}), \quad (\text{B5})$$

D being some operator which is a function of the lattice Laplacian Δ . Here, the lattice Laplacian Δ is defined as,

$$\Delta f(\vec{x}) \equiv - \sum_{i=1}^d [f(\vec{x} + \hat{e}_i) + f(\vec{x} - \hat{e}_i) - 2f(\vec{x})], \quad (\text{B6})$$

with $\{\hat{e}_i\}$ denoting the unit vectors along the Cartesian directions and f some field defined on the lattice. (In the continuum limit, Δ can be replaced by $-\nabla^2$.) The Euler-Lagrange equation then, takes the form,

$$D(\Delta)S(\vec{x}) + u(S^2(\vec{x}) - 1)S(\vec{x}) = 0. \quad (\text{B7})$$

The example mentioned above corresponds to

$$\sum_{\vec{y}} \tilde{V}(\vec{x} - \vec{y}) S(\vec{y}) = -a \Delta S(\vec{x}) + b \Delta^2 S(\vec{x}) + \dots \quad (\text{B8})$$

The Euler Lagrange equation for this finite ranged system reads

$$\begin{aligned} -a \Delta S(\vec{x}) + b \Delta^2 S(\vec{x}) + \dots + \mu S(\vec{x}) \\ + u(S^2(\vec{x}) - 1)S(\vec{x}) = 0. \end{aligned} \quad (\text{B9})$$

-
- [1] A. Mesaros, K. Fujita, H. Eisaki, S. Uchida, J. C. Davis, S. Sachdev, J. Zaanen, M. J. Lawler, and E.-A. Kim, *Science* **333**, 426 (2011).
 - [2] M. B. Salamon and M. Jaime, *Rev. Mod. Phys.* **73**, 583 (2001).
 - [3] B. Kalisky, J. R. Kirtley, J. G. Analytis, J.-H. Chu, A. Vailionis, I. R. Fisher, and K. A. Moler, *Phys. Rev. B* **81**, 184513 (2010).
 - [4] J. R. Kirtley, B. Kalisky, L. Luan, and K. A. Moler, *Phys. Rev. B* **81**, 184514 (2010).
 - [5] J. M. Tranquada, B. J. Sternlieb, J. D. Axe, Y. Nakamura, and S. Uchida, *Nature* **375**, 561 (1995).
 - [6] K. Yamada, C. H. Lee, K. Kurahashi, J. Wada, S. Wakimoto, S. Ueki, H. Kimura, Y. Endoh, S. Hosoya, G. Shirane, et al., *Phys. Rev. B* **57**, 6165 (1998).
 - [7] S. R. White and D. J. Scalapino, *Phys. Rev. Lett.* **80**, 1272 (1998).
 - [8] J. Zaanen and O. Gunnarsson, *Phys. Rev. B* **40**, 7391 (1989).
 - [9] Kazushige and Machida, *Physica C: Superconductivity* **158**, 192 (1989).
 - [10] V. Emery and S. Kivelson, *Physica C: Superconductivity* **209**, 597 (1993).
 - [11] A. A. Koulakov, M. M. Fogler, and B. I. Shklovskii, *Phys. Rev. Lett.* **76**, 499 (1996).
 - [12] M. P. Lilly, K. B. Cooper, J. P. Eisenstein, L. N. Pfeiffer, and K. W. West, *Phys. Rev. Lett.* **82**, 394 (1999).
 - [13] R. Du, D. Tsui, H. Stormer, L. Pfeiffer, K. Baldwin, and K. West, *Solid State Communications* **109**, 389 (1999).
 - [14] D. G. Ravenhall, C. J. Pethick, and J. R. Wilson, *Phys. Rev. Lett.* **50**, 2066 (1983).
 - [15] G. Watanabe, T. Maruyama, K. Sato, K. Yasuoka, and T. Ebisuzaki, *Phys. Rev. Lett.* **94**, 031101 (2005).
 - [16] M. Seul and R. Wolfe, *Phys. Rev. A* **46**, 7519 (1992).
 - [17] A. D. Stoycheva and S. J. Singer, *Phys. Rev. E* **65**, 036706 (2002).

- [18] G. Malescio and G. Pellicane, *Nat Mater* **2**, 97 (2003).
- [19] G. Malescio and G. Pellicane, *Phys. Rev. E* **70**, 021202 (2004).
- [20] M. A. Glaser, G. M. Grason, R. D. Kamien, A. Komrlj, C. D. Santangelo, and P. Ziherl, *EPL (Europhysics Letters)* **78**, 46004 (2007).
- [21] C. J. Olson Reichhardt, C. Reichhardt, and A. R. Bishop, *Phys. Rev. Lett.* **92**, 016801 (2004).
- [22] J. Zaanen, *Nature* **404**, 714 (2000).
- [23] S. A. Kivelson, I. P. Bindloss, E. Fradkin, V. Oganessian, J. M. Tranquada, A. Kapitulnik, and C. Howald, *Rev. Mod. Phys.* **75**, 1201 (2003).
- [24] B. Różycki, T. R. Weikl, and R. Lipowsky, *Phys. Rev. Lett.* **100**, 098103 (2008).
- [25] S. W. Hui and N. B. He, *Biochemistry* **22**, 1159 (1983).
- [26] K. L. Babcock and R. M. Westervelt, *Phys. Rev. A* **40**, 2022 (1989).
- [27] A. Giuliani, J. L. Lebowitz, and E. H. Lieb, *Phys. Rev. B* **76**, 184426 (2007).
- [28] A. Vindigni, N. Saratz, O. Portmann, D. Pescia, and P. Politi, *Phys. Rev. B* **77**, 092414 (2008).
- [29] B. Ma, B. Yao, T. Ye, and M. Lei, *Journal of Applied Physics* **107**, 073107 (2010).
- [30] M. Seul and D. Andelman, *Science* **267**, 476 (1995).
- [31] A. Giuliani, J. L. Lebowitz, and E. H. Lieb, *Phys. Rev. B* **74**, 064420 (2006).
- [32] C. Ortix, J. Lorenzana, and C. Di Castro, *Phys. Rev. B* **73**, 245117 (2006).
- [33] I. Daruka and Z. Gulácsi, *Phys. Rev. E* **58**, 5403 (1998).
- [34] D. G. Barci and D. A. Stariolo, *Phys. Rev. B* **79**, 075437 (2009).
- [35] If we do not have any pole or branch point of the Fourier space correlation function, the form of the real space correlation function is governed by the endpoints of the k -space integration. Therefore, in the continuum, no finite modulation length is allowed. The same is true for the correlation length.
- [36] R. J. Elliott, *Phys. Rev.* **124**, 346 (1961).
- [37] M. E. Fisher and W. Selke, *Phys. Rev. Lett.* **44**, 1502 (1980).
- [38] R. B. Griffiths, *Fundamental problems in statistical mechanics VII* pp. 69–110 (1990).
- [39] An initial and far more cursory treatment appeared in Z. Nussinov, *arXiv:cond-mat/0506554* (2005), unpublished.
- [40] Z. Nussinov, *Phys. Rev. B* **69**, 014208 (2004).
- [41] S. Chakrabarty and Z. Nussinov, *Phys. Rev. B* **84**, 144402 (2011).
- [42] See Eq. (C29) of Ref. [40].
- [43] W. Selke, *Phys. Rep.* **170**, 213 (1988).
- [44] Z. Nussinov, J. Rudnick, S. A. Kivelson, and L. N. Chayes, *Phys. Rev. Lett.* **83**, 472 (1999).
- [45] L. Chayes, V. Emery, S. Kivelson, Z. Nussinov, and G. Tarjus, *Physica A: Statistical Mechanics and its Applications* **225**, 129 (1996).
- [46] T. R. Kirkpatrick and D. Thirumalai, *Journal of Physics A: Mathematical and General* **22**, L149 (1989).
- [47] Z. Nussinov, *arXiv:cond-mat/0105253* (2001) – in particular, see footnote [20] therein for the Ising ground states.
- [48] S. Chakrabarty and Z. Nussinov, *Phys. Rev. B* **84**, 064124 (2011).
- [49] An $O(n)$ system is one for which the order parameter $\vec{S}(\vec{x})$ has n components normalized as $\vec{S}(\vec{x}) \cdot \vec{S}(\vec{x}) = n$. The large n limit of this system is equivalent to the spherical model where the spins are constrained only by the relation $\sum_{\vec{x}} (S(\vec{x}))^2 = N$, where N is the number of lattice sites. See H. E. Stanley, *Phys. Rev.* **176**, 2, 718 (1968).
- [50] H. E. Stanley, *Phys. Rev.* **176**, 718 (1968).
- [51] T. H. Berlin and M. Kac, *Phys. Rev.* **86**, 821 (1952).
- [52] P. Bak and J. von Boehm, *Phys. Rev. B* **21**, 5297 (1980).
- [53] A. Gendiar and T. Nishino, *Phys. Rev. B* **71**, 024404 (2005).
- [54] S. Redner and H. E. Stanley, *J. Phys. C* **10**, 4765 (1977).
- [55] S. Redner and H. E. Stanley, *Phys. Rev. B* **16**, 4901 (1977).
- [56] J. Oitmaa, *J. Phys. A* **18**, 365 (1985).
- [57] D. Mukamel, *J. Phys. A* **10**, L249 (1977).
- [58] R. M. Hornreich, M. Luban, and S. Shtrikman, *Phys. Rev. Lett.* **35**, 1678 (1975).
- [59] K. Zhang and P. Charbonneau, *Phys. Rev. B* **83**, 214303 (2011).
- [60] P. Bak, *Reports on Progress in Physics* **45**, 587 (1982).
- [61] We thank Michael Ogilvie for prompting us to think about this generalization.
- [62] B. D. Josephson, *Phys. Lett.* **21**, 6, 608 (1966).
- [63] H. Thomas, *Nonlinear dynamics in solids* (Springer-Verlag, 1992).
- [64] D. Hu, P. Ronhovde, and Z. Nussinov, *arXiv:cond-mat/1008.2699* (2010).
- [65] J. C. Sprott, *American Journal of Physics* **68**, 758 (2000).
- [66] The $O(n)$ normalization conditions imposes $N_q^2 + 1$ constraints [N_q^2 constraints to ensure no contribution from the non-zero wave-vector modes and one constraint to ensure that the contribution from the zero wave-vector modes results in $\vec{S}_0(\vec{x}) \cdot \vec{S}_0(\vec{x}) = n$] on the set $\{\vec{a}_m\}$ which is described by $2N_q n$ real numbers. Therefore, to be able to find a state characterized by wave-vectors that satisfy the Fourier space Euler-Lagrange equations, we require that such a state must be described by at most \mathcal{M} wave-vectors, where \mathcal{M} is given by,
- $$N_q \leq \mathcal{M} = \left[n + \sqrt{n^2 - 1} \right], \quad (10)$$
- where $[x]$ represents the greatest integer less than or equal to x .
- [67] Y. Pomeau and P. Manneville, *Communications in Mathematical Physics* **74**, 189 (1980), ISSN 0010-3616.
- [68] J. Schmalian and P. G. Wolynes, *Phys. Rev. Lett.* **85**, 836 (2000).
- [69] T. Park, Z. Nussinov, K. R. A. Hazzard, V. A. Sidorov, A. V. Balatsky, J. L. Sarrao, S.-W. Cheong, M. F. Hundley, J.-S. Lee, Q. X. Jia, et al., *Phys. Rev. Lett.* **94**, 017002 (2005).
- [70] S. Pankov and V. Dobrosavljević, *Phys. Rev. Lett.* **94**, 046402 (2005).
- [71] J. W. Clark, M. V. Zverev, and V. A. Khodel, *arXiv:cond-mat.str-el/1203.3201* (2012).
- [72] D. Ma, A. D. Stoica, and X.-L. Wang, *Nat Mater* **8**, 30 (2009).
- [73] H. Zhang, C.-X. Liu, X.-L. Qi, X. Dai, Z. Fang, and S.-C. Zhang, *Nat. Phys.* **5**, 438 (2009).
- [74] C. M. Varma, Z. Nussinov, and W. van Saarloos, *Physics Reports* **361**, 267 (2002).
- [75] P. Coleman, C. Pépin, Q. Si, and R. Ramazashvili, *Journal of Physics: Condensed Matter* **13**, R723 (2001).